

**A MICROMECHANICAL PROCEDURE TO CHARACTERIZE THE
EFFECT OF INTERFACE IN FIBROUS COMPOSITES AND BRAIN
WHITE MATTER**

A Thesis
Submitted to the Graduate Faculty
of the
North Dakota State University
of Agriculture and Applied Science

By

Ataur Rahiman Syed

In Partial Fulfillment of the Requirements
for the Degree of
MASTER OF SCIENCE

Major Department:
Mechanical Engineering

April 2012

Fargo, North Dakota

North Dakota State University
Graduate School

Title

A MICROMECHANICAL PROCEDURE TO CHARECTERIZE THE EFFECT OF INTERFACE
IN FIBROUS COMPOSITES AND BRAIN WHITE MATTER

By

ATAUR RAHIMAN SYED

The Supervisory Committee certifies that this *disquisition* complies with North Dakota State University's regulations and meets the accepted standards for the degree of

MASTER OF SCIENCE

SUPERVISORY COMMITTEE:

DR GHODRAT KARAMI

Chair

DR. FARDAD AZARMI

DR.SUMATHY KRISHNAN

DR.ACHINTYA BEZBARUAH

Approved:

04/30/2012

Date

Dr. ALAN KALMAYER

Department Chair

ABSTRACT

A micromechanics computational algorithm for fibrous composites including fiber, matrix and interface is introduced to study the impact of interface on composite behavior. The domains are modeled by finite elements with the interface simulated by cohesive zone elements. The constitutive of the cohesive zone behavior is extracted from the experimental traction-separation relations. By implementing this model under different loading conditions, significant difference in the composite behavior is observed with different cohesive zone laws and different fiber waviness. The composite strength and stiffness for the examined cases are compared to experimental data and are in good agreement.

The procedure is then extended to study the impact of adhesion on brain axonal injury. The constituents of the brain tissue are modeled as linear viscoelastic materials. This micromechanical model has been implemented to study the impact of adhesion and waviness on the stiffness and viscous behavior of brain tissue with respect to time.

ACKNOWLEDGEMENTS

The author would like to thank Air Force Office of Scientific Research (AFOSR) and NSF National Research Foundation (NSF) for financial support of this work.

I am heartily thankful to my supervisor, Dr. Ghodrat Karami, whose encouragement, guidance and support from the initial to the final level enabled me to develop an understanding of the research project. His extensive knowledge and logical ideas to resolve complex problems have been of great direction for me. His patience to make me understand, continuous encouragement and personal recommendation have provided a good support for the present thesis. I also thank my graduate committee members, for allocating time in their busy schedules to serve on my committee.

My special gratitude is due to my family, friends and colleagues for their support and companionship. Without their faith and belief in me it would have been preposterous for me to complete this tremendous work.

TABLE OF CONTENTS

ABSTRACT.....	iii
ACKNOWLEDGEMENTS.....	iv
LIST OF TABLES.....	viii
LIST OF FIGURES.....	ix
NOMENCLATURE	xiii
CHAPTER 1. INTRODUCTION TO ADHESION IN COMPOSITES, BIOMATERIALS, AND RESEARCH OBJECTIVE.....	1
1.1 Adhesion in Composites.....	1
1.2 Adhesion in Biomaterials.....	4
1.3 Research Objective.....	8
CHAPTER 2. DEVELOPMENTS IN MICROMECHANICS OF ADHESION MODELING.....	10
CHAPTER 3. DEVELOPMENT AND MODELING OF A PERIODIC UNIT CELL FOR MICROMECHANICAL ANALYSIS WITH ADHESION.....	12
3.1 Composite Materials with Undulated Fiber.....	12
3.2 Unit Cell Geometry.....	14
3.3 Interface Thickness for Adhesion Modeling.....	15
3.4 Incorporation of Cohesive Zone Elements.....	17
3.5 Loading and Periodicity Constraints.....	20
3.6 Periodicity and Rigid Body Motion Constraints.....	22
CHAPTER 4. MICROMECHANICAL EVALAUTION OF MATERIAL DEGRADATION OF FIBROUS COMPOSITES DUE TO INTERFACIAL FAILURE.....	23
4.1 Introduction.....	23

4.2 Material Input of Adhesion and Constituents.....	24
CHAPTER 5. COMPARISION OF MICROMECHANICAL MATERIAL DEGRADATION OF UNIT CELLS WITH DIFFERENT ADHESION BEHAVIOR AND UNDULATIONS.....	
5.1 Material Degradation of Unidirectional Carbon/Epoxy Composite with Mixed Mode-Bilinear Traction Separation Based Cohesive Zone.....	26
5.2 Material Degradation of Wavy Glass/Epoxy Composite with Mixed Mode-Bilinear Traction Separation Based Cohesive Zone.....	29
5.3 Comparison of Material Degradation of Unidirectional Glass/Epoxy Composite Using Bilinear and Exponential Traction Separation Cohesive Zone Laws.....	33
5.4 Comparison of Material Degradation of Glass/Epoxy Composite with Different Waviness of Fiber.....	36
CHAPTER 6. EFFECT OF ADHESION ON VISCOELASTIC CHARACTERIZATION OF MECHANICAL PROPERTIES OF BRAIN WHITE MATTER.....	
6.1 Introduction.....	43
6.2 Relaxation Loading.....	44
6.3 The Material Data for Adhesion, Axons, and Matrix.....	45
CHAPTER 7. COMPARISION OF MICROMECHANICAL VISCOELASTIC BEHAVIOR OF UNIT CELLS DUE TO THE EFFECT OF DIFFERENT ADHESION AND UNDULATIONS.....	
7.1 Impact of Adhesion on the Viscous Behavior of Axons and Matrix in a Unidirectional Brain Composite Unit Cell with Bilinear Traction Separation Based Cohesive Zone.....	47
7.2 Impact of Adhesion on the Viscous Behavior of Axons and Matrix in a Brain Composite Unit Cell with a Constant Waviness (A/L) of 1.0684 Using Bilinear Traction Separation Based Cohesive Zone.....	52
7.3 Impact of Waviness on the Viscous Behavior of Axons and Matrix in a Brain Composite Unit Cell with a Constant Adhesion Strength (A1) Using Bilinear Traction Separation Based Cohesive Zone.....	56

CHAPTER 8. CONCLUSIONS AND SUGGESTIONS FOR FURTHER RESEARCH.....	61
8.1 Conclusions.....	61
8.2 Suggestions for Further Research.....	64
REFERENCES.....	65

LIST OF TABLES

<u>Table</u>	<u>Page</u>
1. Mechanical properties of the fiber and matrix [42].....	25
2. Mechanical properties of interface elements for Composite #1 [41].....	25
3. Mechanical properties of interface elements for Composite #2 [40].....	25
4. Comparison of initial stiffness and strength of unidirectional carbon/ epoxy composite calculated using the proposed method with the available literature data.....	31
5. Viscoelastic property of axon material [63].....	46
6. Viscoelastic behavior of ECM material.....	46
7. Mechanical properties of interface elements for the study of axon-ECM adhesion [38, 52, 71].....	46

LIST OF FIGURES

<u>Figure</u>	<u>Page</u>
1. (a) Schematic representation hexagonal periodic distribution of fibers in an epoxy matrix with a periodic microstructure (d =fiber diameter, w =width of unit cell, h : height of unit cell= $\sqrt{3} w$); (b) Schematic representation of hexagonal wavy fiber distribution (Sinusoidal curve with amplitude, A ; Peak to peak distance, $2A$; and wavelength, λ).....	13
2. Schematic representation of the adhesion between axon and ECM in brain tissue using the cohesive zone element with traction separation response as adhesion.....	15
3. (a) Mixed mode behavior of cohesive element for glass/epoxy and carbon/epoxy composite. (b) Bilinear cohesive zone law for glass/epoxy composite. (c) Exponential cohesive zone law for glass/epoxy composite.....	18
4. Independent mode bilinear behavior of cohesive element for Axon-ECM composite with three different traction-separation data.....	20
5. Schematic of the possible load scenarios.....	21
6. Tensile stress-strain distribution in fiber, matrix, and composite due to the applied strain in direction 2-2 in a unidirectional carbon/epoxy composite model of $V_F/V=0.4$	27
7. Shear stress-strain distribution in fiber, matrix, and composite due to the applied strain in direction 1-2 in a unidirectional carbon/epoxy composite model of $V_F/V=0.4$	29
8. Compressive stress-strain distribution in fiber, matrix, and composite due to the applied strain in direction 2-2 in a unidirectional carbon/epoxy composite model of $V_F/V=0.4$	30
9. Tensile stress-strain distribution in fiber, matrix, and composite due to the applied strain in direction 1-1 in a glass/epoxy composite model with waviness ($A/L=0.085$) of $V_F/V=0.4$	31
10. Tensile stress-strain distribution in fiber, matrix, and composite due to the applied strain in direction 2-2 in a glass/epoxy composite model with waviness ($A/L=0.085$) of $V_F/V=0.4$	33

<u>Figure</u>	<u>Page</u>
11. Compressive stress-strain distribution in fiber, matrix, and composite due to the applied strain in direction 1-1 in a glass/epoxy composite model with waviness ($A/L=0.085$) of $V_F/V=0.4$	34
12. Shear stress-strain distribution in fiber, matrix, and composite due to the applied strain in direction 1-2 in a glass/epoxy composite model with waviness ($A/L=0.085$) of $V_F/V=0.4$	35
13. Tensile stress-strain distribution in unidirectional glass/epoxy composite models of $V_F/V=0.4$ due to the applied strain in direction 2-2 with two different (bilinear and exponential) traction-separation behaviors.....	36
14. Compressive stress-strain distribution in unidirectional glass/epoxy composite models of $V_F/V=0.4$ due to the applied strain in direction 2-2 with two different (bilinear and exponential) traction-separation behaviors.....	37
15. Shear stress-strain distribution in unidirectional glass/epoxy composite models of $V_F/V=0.4$ due to the applied strain in direction 1-2 with two different (bilinear and exponential) traction-separation behaviors.....	38
16. Tensile stress-strain distribution in glass/epoxy composite models of $V_F/V=0.4$ due to the applied strain in direction 1-1 for three different waviness ($A/L=0.0853, 0.121, 0.179$).....	39
17. Tensile stress-strain distribution in glass/epoxy composite models of $V_F/V=0.4$ due to the applied strain in direction 2-2 for four different waviness ($A/L=0, 0.0853, 0.121, 0.179$).....	40
18. Compressive stress-strain distribution in glass/epoxy composite models of $V_F/V=0.4$ due to the applied strain in direction 1-1 for three different waviness ($A/L=0.0853, 0.121, 0.179$).....	41
19. Shear stress-strain distribution in glass/epoxy composite models of $V_F/V=0.4$ due to the applied strain in direction 1-2 for four different waviness ($A/L=0, 0.0853, 0.121, 0.179$).....	42
20. Variation of shear stress with respect to time due to the applied constant strain in direction 1-2 with three different adhesion properties in a unidirectional brain unit cell model of $V_F/V=0.53$	48
21. Variation of tensile stress with three different adhesion properties in axons, matrix, and brain composite tissue due to the applied constant strain in direction 2-2 in a unidirectional brain unit cell model of $V_F/V=0.53$	49

<u>Figure</u>	<u>Page</u>
22. Variation of stiffness with three different adhesion properties in axons, matrix, and brain composite tissue due to the applied constant strain in direction 1-2 in a unidirectional brain unit cell model of $V_F/V=0.53$	49
23. Illustration of the tensile stresses (S_{22}) developed in the (a) unidirectional tissue unit cell with A_1 (weak) adhesion; (b) unidirectional tissue unit cell with A_2 (strong) adhesion; and (c) unidirectional tissue unit cell with 100% bonding between axon and matrix when subjected to an average constant strain of 0.3% along 2-2 direction.....	50
24. Illustration of the shear stresses (S_{12}) developed in the (a) unidirectional tissue unit cell with A_1 (weak) adhesion; (b) unidirectional tissue unit cell with A_2 (strong) adhesion; and (c) unidirectional tissue unit cell with 100% bonding between axon and matrix when subjected to an average constant strain of 0.3% along 1-2 direction.....	51
25. Illustration of the compressive stresses (S_{22}) developed in the (a) unidirectional tissue unit cell with A_1 (weak) adhesion; (b) unidirectional tissue unit cell with A_2 (strong) adhesion; and (c) unidirectional tissue unit cell with 100% bonding between axon and matrix when subjected to an average constant strain of 0.3% along 2-2 direction.....	52
26. Variation of axial stress with respect to time due to the applied constant strain in direction 1-1 with two different adhesion properties in a brain unit cell model with waviness ($A/L=1.0684$) of $V_F/V=0.53$	53
27. Variation of shear stress with respect to time due to the applied constant strain in direction 1-2 with two different adhesion properties in a brain unit cell model with waviness ($A/L=1.0684$) of $V_F/V=0.53$	53
28. Illustration of the shear stresses (S_{12}) developed in the (a) tissue unit cell with undulation, $A/L=1.0684$ with A_1 (weak) adhesion; (b) tissue unit cell with undulation, $A/L=1.0684$ with A_2 (strong) adhesion when subjected to an average constant strain of 0.3% along 1-2 direction, which is perpendicular to the fiber direction (load case 5). The deformed shape of the axon with respect to its original shape is also shown in (c).....	54
29. Variation of compressive stress with respect to time due to the applied constant strain in direction 1-1 with two different adhesion properties in a brain unit cell model with waviness ($A/L=1.1310$) of $V_F/V=0.53$	56

30. Variation of axial stress with respect to time due to the applied constant strain in direction 1-1 with three different waviness ($A/L=1.0684, 1.1310, 1.1947$) in a brain unit cell model with a weak adhesion property (A_1) of $V_F/V=0.53$57

31. Illustration of the axial stresses (S_{11}) developed in the (a) tissue unit cell with undulation, $A/L=1.0684$ with A_1 (weak) adhesion; (b) tissue unit cell with undulation, $A/L=1.131$ with A_1 (weak) adhesion; and (c) tissue unit cell with undulation, $A/L=1.1947$ with A_1 (weak) adhesion when subjected to an average constant strain of 0.3% along longitudinal axon direction (load case 1).....58

32. Variation of compressive stress with respect to time due to the applied constant strain in direction 1-1 with three different waviness ($A/L=1.0684, 1.1310, 1.1947$) in a brain unit cell model with a weak adhesion property (A_1) of $V_F/V=0.53$58

33. Variation of shear stress with respect to time due to the applied constant strain in direction 1-2 with three different waviness ($A/L=1.0684, 1.1310, 1.1947$) in a brain unit cell model with a weak adhesion property (A_1) of $V_F/V=0.53$59

NOMENCLATURE

1. RVE....Representative Volume Element
2. RUC....Repetitive Unit Cell
3. ECM... Extra Cellular Matrix
4. FEA....Finite Element Analysis
5. FA....Focal Adhesion
6. CNS...Central Nervous System
7. DAI...Diffuse Axonal Injury

CHAPTER 1. INTRODUCTION TO ADHESION IN COMPOSITES, BIOMATERIALS, AND RESEARCH

OBJECTIVE

1.1 Adhesion in Composites

The fiber-matrix interface plays an important role in defining key properties of the composite materials such as stiffness, strength and fracture behavior [1]. In general the global mechanical properties of the material are affected by local failures that include particle (or fiber) splitting, interfacial debonding and matrix cracking [2]. The adhesion behavior alters with different combination of materials and thereby directly impacts the load transfer behavior between matrix and fiber. The interface between non-reactive polymers considers numerous factors. Elastomers and thermoplastics have different interface mechanisms. The interface between polymers is controlled by the entanglement between the two materials. If the materials are essentially insoluble in each other the interface between them will be narrow. The expected interface will be lower than in the situations where the materials have broad interface resulting in stronger bonding. In some cases such interface properties can be increased greatly by fiber sizing techniques [3].

Adhesion test is mainly based on the fracture mechanics tests and crack propagation concepts. Pull out test is a widely known method for measuring the adhesion [2]. In fracture mechanics tests, especially for the fiber reinforced composites two important modes are characterized; crack opening mode and shear mode. In modeling, interfacial properties have been evaluated in a number of different ways. By assuming a continuous region with its material properties distinct from the matrix and fiber has been

a general approach to model the interaction. However, evaluation of the material properties of this domain is very difficult considering the geometry and scale [4]. The effects of damage due to interfacial decohesion on overall mechanical properties of the composite material have been studied by various authors [5,6]. A number of numerical models have been proposed and developed over the years to simulate interfacial behavior in composite microstructures. One such method to simulate interfacial behavior is the cohesive zone model, where the interfaces are assumed to be comprised of nonlinear springs of negligible thickness with a specific traction-displacement law. The approach was introduced to analyze interface failure at metal-ceramic interfaces by Needleman [7, 8] and has been used by several researchers including Tvergaard [9], Ghosh et al.[10], Allen et. al.[11, 12], Lissenden et. al.[13], Geubelle [14] and Ortiz et al.[15, 16], to study the damage evolution in micromechanical problems. Tvergaard [9] and Ghosh et. al. [10] have used the cohesive zone model to simulate interface fracture in two dimensional problems, while Ortiz and Pandolfi [16], Scheider [17], Segurado and LLorca [18] and Foulk et. al.[11] have applied it to model failure in 3D problems. In their work, Ortiz and Pandolfi [16] have developed 3D cohesive elements with irreversible cohesive laws to simulate dynamically growing cracks and compared it with experimental results for a drop-weight dynamic fracture test. Scheider [17] has described the numerical aspects of the implementation of the cohesive model, based on the traction-separation laws developed by Needleman [7, 8]. Segurado and LLorca et.al [18] have implemented the cohesive zone model to solve the problem of decohesion in sphere-reinforced composites and Foulk et.al.[11] have implemented the model to study the matrix cracking and interfacial debonding in a unidirectional metal matrix composite using a simplified

representative volume element (RVE). Ananth and Chandra [19] have used a spring layer model in their numerical analysis and they have found the stress and debonding criterion as well as friction in relative sliding between fiber and matrix. In their method the approach has been to model the push-out test as interfacial effect by representing the interface region with a set of springs. Although this might be far from the real framework of continuum interface property in many situations, it can be looked as a simplified solution for numerical implementation. In all these models, special cohesive interface elements, defined by a constitutive equation, are created between the continuum elements. The cohesive elements open with damage initiation and lose their stiffness at failure so that the continuum elements are disconnected. Cohesive elements have been made of two quadrilateral surfaces connecting brick elements [17] or have been comprise of two triangular surfaces connecting tetrahedral elements [16, 18]. These works primarily discuss the finite element aspects of the implementation of the cohesive zone for 3D microstructures (RVE) to simulate interfacial debonding and validate it for specified boundary value problems. There has been limited work done in literature to address the effect of interface on the modeling procedure of material characterization of fiber reinforced composites. Analytical approaches to implement cohesive zone are been carried out by some other researchers [20].

In actual composite microstructures, the fibers are not perfectly bonded with the surrounding matrix and defects such as undulation of fibers that occur during the fabrication process have adverse influence on the rate of degradation of stiffness and compressive strength of the fiber reinforced composite. In composite microstructures, the fiber-matrix interface is developed because of the chemical reactions between the two

continuum materials. Micromechanical modeling of the composite is a suitable and useful tool to study the impact of interface on mechanical property of composites for different load cases and combinations of materials and geometries [21]. In this study, a micromechanical modeling procedure in conjunction with traction-separation based cohesive zone which acts as fiber-matrix interface is proposed for straight and wavy fibers. The cohesive element uses the constitutive equation as defined by the bilinear model [15, 16] for representing the interface. It has been observed that cohesive zone has a dominant role in the degradation of material property in transverse, compression and shear loading perpendicular to fiber direction. The stiffness change of the composites as a function of the stress distribution in the composite versus the applied strain is reported for two different unit cell geometries.

1.2 Adhesion in Biomaterials

The study of Axon-ECM adhesions are dominant for brain functions such as memory and learning [22-24]. Biologically, brain matter consists of a base matrix (neurons and extracellular components: gray matter) crossed by a network of neural tracts (or axonal fibers) in the so-called white matter. The nervous brain tissue consists of three components: an outer implantable sheath forming a conduit, an extracellular matrix within the lumen, and living stretch grown axons embedded within the extracellular matrix. The white matter, one of the key areas of central nervous system (CNS), is composed of myelinated axons, the supporting glia cell network and the innervating vascular system. The formation of nervous system at the early stages is by the elongation of neural axons to establish and maintain connections through the formation of axon-axon and axon-ecm adhesions.

Considerable efforts have been made from past two decades to understand the impact of cell adhesion in different biological processes. [25-27]. The cell fate is highly dependent on the cell adhesion because of the signaling behavior between the surrounding environment and the cell [28]. Adhesion of cell to the surface occurs because of distinct interactions between receptor and ligand molecules on the cell membrane and the substrate respectively which makes cell adhesion a complicated dynamic biological process. The structure between the actin and ECM are considered to be the area of strongest adhesion known as Focal Adhesions (FA) [29] which are formed by the rapid association of receptors with cytoskeleton. The important process in the growth of FAs is the clustering of receptors which results in a non uniform adhesive zone [30, 31]. Several theoretical models have been implemented to better understand the biophysics of adhesion in cells [32-35]. A 1-D peeling model has been developed by Evans (1985a, b) to study the mechanics in cell adhesion by assuming adhesive zone to be discretely or continuously distributed [36, 37]. In a continuous distribution, the force required to separate the membrane is equal to the force generated by adhesion but for discrete attachments, it was observed that the force for separation is much larger than the force produced during attachment process. The affect of cell-ecm strength because of clustering in receptors was studied by Ward and Hammer (1993) [38] and they have predicted that the formation of FAs increases the adhesive strength. Ward et al. (1994) evaluated the rate of separation of a surface by using Dembo et al. (1988) method and concluded that detachment was a factor of the bond density of receptor, but the mechanical and chemical characteristics of receptor–ligand bindings can impact the strength of cell adhesion [39, 40].

During the initial studies, cell adhesion was considered as linear elastic springs, with a defined elasticity though the mechanical response of the bindings is usually not linear. Also, the detachment of the bindings is based on the changes of ligand and receptor [41-43] which makes the linear behavior as a simple assumption to analyze the complex deformation of the bonds between cytoskeleton and cell membrane. The force-extension relationship of adhesion is highly nonlinear as per numerical and experimental studies, specifically at the threshold level of the bond [44, 45]. Hence, it is very important to study if the nonlinearity of the force-extension of the bindings will affect the behavior of adhesion in cell. It has been analyzed in recent research that the nonlinear response of bonds at micron and nano level can highly affect the fracture/adhesive strength in material with two contact surfaces [46-51]. Due to limited studies on the non-linear behavior of the receptor-ligand bindings, it has become significant to understand the biological and mechanical response in cell adhesion. A nonlinear one-dimensional peeling model was introduced by Kong et al. 2007 and the impact of nonlinear response of bindings on the adhesive behavior was analyzed with three types of bindings [52]. In their study, they found that the growth of adhesive strength is highly dependent on the nonlinear force-extension behavior of bonds and especially at the outer border of the adhesion region. The cell adhesion strength is not sensitive with changing bond density. In their study, it has been assumed that adhesive stresses act perpendicular to the surface. The surface is divided into free zone (no adhesive stresses) and adhesive zone (with attractive stresses). The surface mechanics for all zones needs to be analyzed separately and then at the interface of the two zones requires continuity of the solutions. In a linear behavior, the cell detaching process initiates when the pressure at the outer edge of the

cell crosses the threshold resulting in the detachment of substrate from the cell [36, 38, 39, 53]. But in the nonlinear model, adhesion continuously resists until the maximum bond force is exceeded with a new criteria for cell detachment. Ward et al., 1994 has also implemented a similar model as of Kong et al., 2007 to understand the kinetics of cell detachment. In their study, clustering of cell surface receptors is an important process for the growth of focal contacts, specialized cell-substrate attachment sites where receptors are simultaneously linked to extracellular ligand and cytoskeletal proteins. In fact, there was a quantitative match between the models used in Ward et al., 1994 and data on the strengthening response of glioma cell adhesion to fibronectin in Lotz et al., 1989. In Lotz et al., 1989, a centrifugal force-based adhesion assay was used for the adhesive strength measurements and the corresponding morphology was visualized by interference reflection microscopy and the cell-substratum adhesion has been quantified using fibroblasts and glioma cells binding to two extracellular matrix proteins, fibronectin and tenascin which are mostly the proteins, integrins and neuron cells found in brain tissue [54, 55].

The injuries related to axons in the white matter have a major contribution to brain in central nervous system (CNS). Diffuse Axonal Injury is a depreating type of injury in brain which is characterized by damage of axons and adhesion molecules at microscopic level within the brain white matter, rostral brainstem and corpus callosum. In depth knowledge of Axon-ECM adhesion and Cell-Cell adhesion in brain is required to understand the response for different mechanical loadings. In this work, a micromechanics computational algorithm for brain tissue including Axon, ECM and adhesion has been introduced.

1.3 Research Objective

The objective of this research work will be a major effort to understand and develop appropriate micromechanical model to study the effect of adhesion in composite and brain tissue. In this thesis, we will develop a micromechanical model by incorporating cohesive zone in a representative volume element which will exhibit the adhesion behavior in composites and brain white matter at microscale level. This method will be first applied to study the effect of adhesion on material response of the composite materials. This analysis will be implemented with two different composite materials ie., Glass-Epoxy and Carbon-Epoxy. The developed repetitive unit cell will be subjected to all possible loading scenarios in which adhesion has a significant impact on the overall material response of the composite. The volume averaged stresses and strains will be captured to calculate the overall material response on the composite in all directions. The calculated results will be then compared with the available literature data to check the level of accuracy for the developed cohesive zone micromechanical model. Two different traction separation models including bilinear and exponential cohesive zone laws will be used to define the behavior of adhesion and the mechanical behavior of the composite will be calculated to study the effect of traction separation model. The principles of micromechanics are also being implemented in biomechanics with huge success. A huge similarity can be found between the brain white matter and a conventional composite material considering the fibrous structure of axons. As brain white matter shows a composite distribution of axons and extracellular matrix, micromechanical unit cells with cohesive zone will be used to analyze the effect of adhesion on the mechanical behavior of brain tissue. In this study we will study the effect of adhesion using hexagonal packing of the representative unit cell as

studies have indicated that regions of brain white matter have a similar packing of axons in ecm. In this study, the impact of adhesion on load transfer characteristics in fiber and matrix will be determined. The impact of cohesive zone models on the material response of composites will be studied in order to verify the appropriate traction separation data. The finite element analysis will be continued to understand the effect of waviness with constant adhesion on the viscous behavior and stiffness of the overall brain tissue. Also, the effect of varying adhesion with constant waviness will be evaluated to understand the material response in different regions of brain.

CHAPTER 2. DEVELOPMENTS IN MICROMECHANICS OF ADHESION MODELING

Micromechanics is accounting for the impact of microstructure properties and behavior on the global behavior of composites. The overall behavior of composite materials can be predicted by the micromechanical methods that have been developed till date. By using energy variation principles, the upper and lower levels of elastic moduli are calculated [56]. A micromechanical theory was developed by Aboudi [57] to calculate the overall material response of composites based on periodic unit cells. Aboudi applied homogeneous boundary conditions to the periodic unit cell models by applying normal tractions on the boundaries. The assumption of plane-remains-plane over-constrains the boundary conditions for the case of shear loading [58] and thereby cannot be considered as periodic boundary conditions. In major research studies, applied boundary conditions were considered as periodic, which is in fact wrong even if results were close to the experimental data. The mechanical behavior of a RUC in a continuum domain should be calculated using the periodicity constraints. The result can be validated if the adjoining unit cells are deformed in the similar fashion as of the RUC analyzed. In order to evaluate damage behavior and mechanical characteristics in composites, periodicity has been assumed by several researchers who have implemented finite elements analysis of the so-called periodic unit cells by using elastic and thermoelastic material properties [59, 60]. Brinson and Lin [61] and Fisher and Brinson [62] have implemented micromechanical analysis of periodic structures and compared the results with the Mori-Tanaka method.

The principles of micromechanics are also being implemented in biomechanics with huge success. The methods from composite field are being transmitted into biomechanics which has led to a major development in studies related to brain injuries. A huge similarity can be found between the brain white matter and a conventional composite material considering the fibrous structure of axons. As brain white matter shows a composite distribution of axons and extracellular matrix, micromechanical unit cells can be used to analyze the behavior. Arbogast and Margulies (1999) have observed that axonal distribution within brainstem is highly oriented which can be modeled as unidirectional composites. Axon undulations are observed in different areas of brain which includes white matter and corona radiata. The effect of undulation on the material response can also be evaluated by using the discussed method. Although researchers in biomechanics utilize micromechanics principles to characterize the biological materials, they are limited to simple formulations. Arbogast and Margulies (1999) have utilized Hashin models to calculate the property of the brain white matter. Implementation of finite element analysis techniques can benefit the accuracy of such solutions [63]. The macroscopic behavior of brain tissue can be determined with such axonal microstructure to predict the injury tolerance by calculating the stress-strains experienced by individual. The characterization of mechanical property of brain tissue has been attempted with the conventional models but has failed to provide the local stress-strain distribution.

CHAPTER 3. DEVELOPMENT AND MODELING OF A PERIODIC UNIT CELL FOR MICROMECHANICAL ANALYSIS WITH ADHESION

In the proposed study, we implement a finite element micromechanical method to evaluate adhesion effect on the degradation of mechanical behavior of the composite and also to determine the load transfer characteristics in fiber and matrix. The RUC is a representative unit cell of the composite, which will be subjected to three load cases. The three load scenarios are assorted by two axial loadings and one transverse shear loading perpendicular to fiber direction. These load scenarios are considered as the most common loading cases to determine the impact of adhesion on the degradation of stiffness of the composite. Periodic conditions with required physical constraints to prevent rigid body movements are implemented on the unit cell. Also, this approach is extended to evaluate the effect of different adhesions on the viscoelastic material behavior of the brain composite model and also to determine the load transfer characteristics in Axon and ECM with three different adhesion behaviors.

3.1 Composite Materials with Undulated Fiber

In fabrication of laminated composites, errors such as the undulation of fibers might occur in filament winding processes which might impact different mechanical properties of the laminate structures (Fig. 1(b)). Therefore assumption of composites with perfectly aligned straight fibers can be ideal. The waviness of fiber in composites produced during the manufacturing process will result in adverse effect on the compressive strength [59]. Analytical and numerical schemes have also been introduced

to study the impact of waviness [21]. The fiber waviness factor has also been measured by experimental procedures [64]. The effect of fiber undulation on mechanical behavior of unidirectional composites under compression has been analyzed by Hsiao and Daniel [65]. Generally waviness is developed because of the geometrical nonuniformity and thus increases material non uniformity in the composite. Such non uniformity in-turn increases the complexities in the structural analysis of composites. The proposed micromechanics method is implemented for a RUC of the fibrous composite with different fiber waviness. Also, the periodic local stresses which are not included in the current structural analysis methods are examined to study the lamina failure.

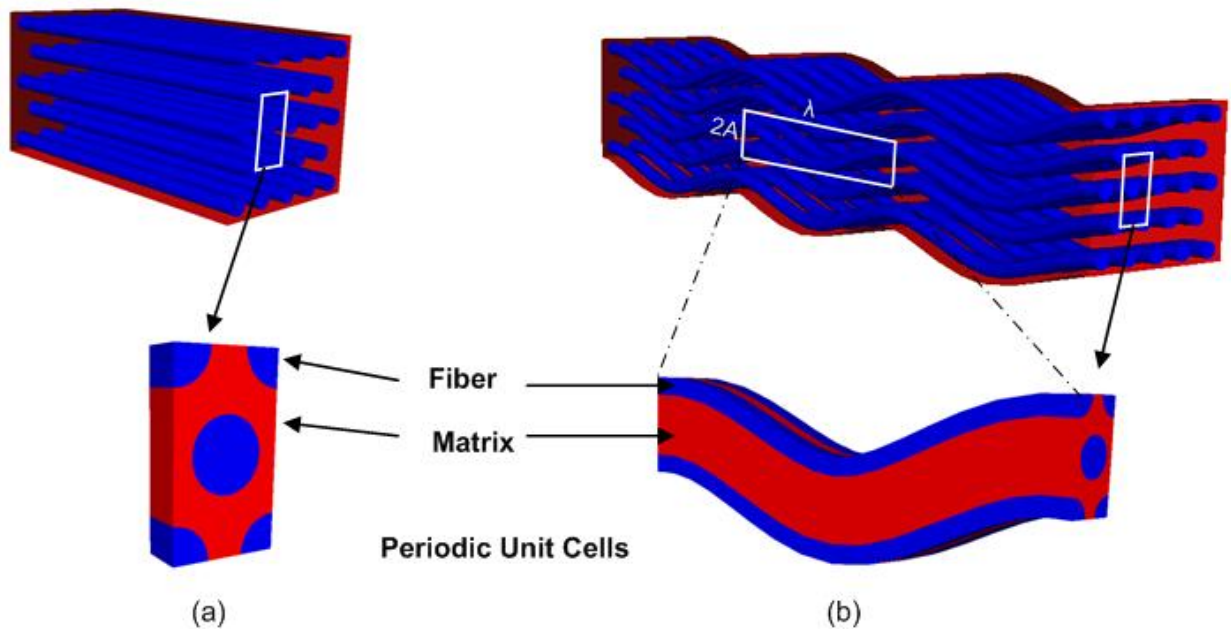


Figure 1. (a) Schematic representation of hexagonal periodic distribution of fibers in an epoxy matrix with a periodic microstructure (d =fiber diameter, w =width of unit cell, h : height of the unit cell= $\sqrt{3} w$); (b) Schematic representation of hexagonal wavy fiber distribution (Sinusoidal curve with amplitude, A ; Peak to peak distance, $2A$; and wavelength, λ).

3.2 Unit Cell Geometry

The micromechanical models for fiber and matrix are developed based on the assumption of hexagonal fiber packing (Fig. 1 and 2) to simulate finite element analysis. The models are created for both straight as well as wavy fibers. The Figs. 1 (a) and (b) show the periodic microstructure of both straight as well as wavy models. In composites, the circular cross sectioned fibers are distributed periodically and are defined by a rectangular unit cell with symmetry lines (Fig. 2). In wavy fibers, the symmetric lines should extrude in the third dimension in order to follow the fiber curvature for a complete periodic unit cell with the initial waviness as sinusoidal. The parameters of the unit cell geometry will include the cross-sectional width (w), the fiber diameter (d), the wavelength L and the amplitude A , where the peak-to-peak amplitude of a sine wave is equal to $2A$. The wavy model for composites implemented in this study is of amplitude/wavelength (A/L) of 0.085, 0.121 and 0.179 and for brain material the wavy model implemented is of amplitude/wavelength (A/L) of 1.0684, 1.1310 and 1.1947. The wavy unit cell is subjected to four different load cases under kinematic boundary conditions for both composite materials and brain material in order to evaluate the effect of interface on the waviness, the degradation of material property of the composite material and on the viscoelastic nature of the brain material. The pairs of nodes on opposite faces of the unit cell are applied with periodic and translational restraints to prevent any rigid body movements. The applied constraints are considered as kinematic boundary conditions that are applied on the unit cell.

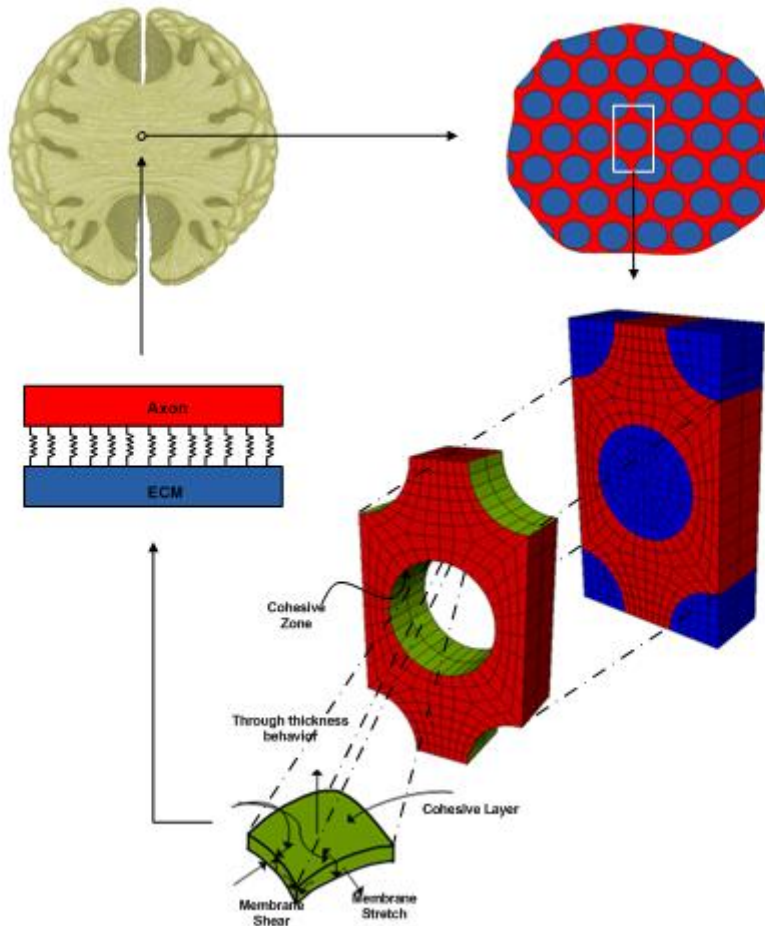


Figure 2. Schematic representation of the adhesion between axon and ECM in brain tissue using the cohesive zone element with traction separation response as adhesion.

3.3 Interface Thickness for Adhesion Modeling

The interface refers to an inhomogeneous region between fiber and matrix within a composite material (Figure 2). Interface areas may be developed due to air gaps (bubbles), mechanical disorder and other inconsistencies [66]. The interface in composites is also resulted due to fiber sizing techniques for special mechanical properties to optimize the performance of composites. A comparatively small volume fraction of interface may have a phenomenal role in evaluating the overall mechanical

behavior of the composite. The challenge in developing a interface model is the evaluation of the size and mechanical behavior of the adhesion area. There are several works still going on to better estimate these properties. In the past, the thickness of a polymer matrix composite interface was estimated to be $30nm-240nm$ [67] and has been accounted in an experiment using the scanning force microscopy [68]. In some of the recent experimental findings which included secondary ion mass spectroscopy [69] and atomic force microscopy [70], it has been suggested that the interface region within polymer matrix composite materials may be even larger upto 1 mm for glass-fiber epoxy composites. In this study the interface thicknesses for both glass/epoxy and carbon/epoxy composite materials are assumed as $1\mu m$.

The interface in brain material is regarded as inhomogeneous axon-ecm binding area in the brain composite material (Figure 2). In our work, we tried to make a connection between the receptor-ligand binding data for cell adhesion from literature [40, 52, 71] and our specific Axon-ECM adhesion in brain tissue. Cell-Adhesion depends on enormous factors like cell membrane, bending modulus, number of integrins, adhesion area and shape of the cell. As there has been no work done to evaluate our specific interface material properties of axon-ecm adhesion in brain tissue, we have calculated the interface properties from the available different kinds of cell-adhesion data which are found in literature. Interestingly, Chan and Odde, 2008 found that the critical stiffness sensed by cells like fibroblasts, neurons and epithelial was of the same order as measured in brain tissue [72]. As previously discussed, we found a close similarity between the Cell-ECM adhesion used by different researchers in literature and we have evaluated the required interface properties for adhesion modeling assuming that the mechanics of cell-

adhesion is same for axon-ecm adhesion in brain tissue. The domains are modeled by finite elements with the interface simulated by cohesive zone elements. The initial stiffness, strength and adhesion energy of interface evaluated are in the range when compared to the published results for different cell-adhesion. In this study, thickness of Cell-Adhesion is considered as 100 nm [73].

3.4 Incorporation of Cohesive Zone Elements

In order to understand the effect of adhesion on the overall material behavior of composite and brain material, it is essential to consider the interface behavior while developing the computation models. The objective of this study is to incorporate cohesive zone elements into micromechanical models and simulate overall material behavior of composite and brain. In order to represent the adhesion between the fiber and matrix, we have used a traction separation based 3D cohesive zone element see Fig.3 and Fig.4 for detailed schematic representation for composites and brain material. The cohesive zone is a defined element in ABAQUS that can mirror the response of a bonded region, similar to adhesion between fiber and matrix, interlaminar in composites. The cohesive element is modeled with a initial stiffness and then developing a damage profile which leads to failure at the adhesion zone. The thickness of the cohesive element is generally considered to be negligible. We used a bi-linear and exponential traction separation based 3D cohesive zone element to represent the interface between the fiber and matrix for composites and bi-linear behavior for brain material [74]. A three-dimensional micromechanical model has been developed to study the fiber-matrix interfacial debonding in composite microstructures [75]. The fiber-matrix adhesion behavior in the parallel and perpendicular directions is studied by a non-linear 3D CZM

with bilinear traction-separation model. Experiments for composites have good agreement when bilinear cohesive zone law is used [76, 77]. The cohesive zone elements have been modeled using ABAQUS [74].

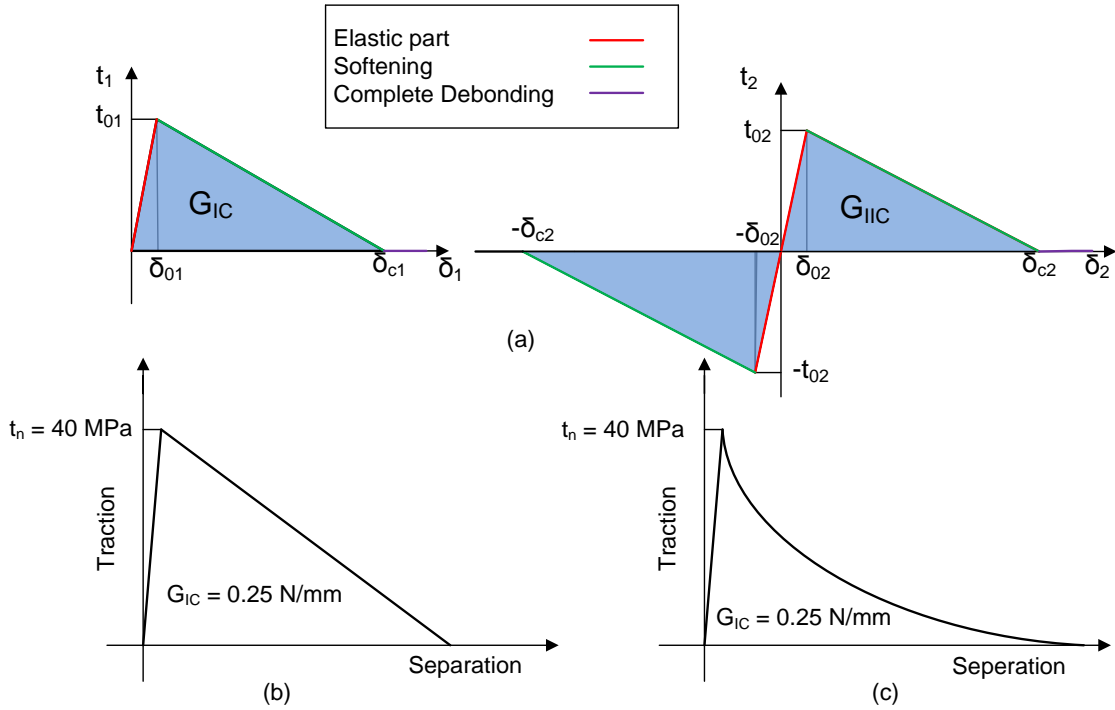


Figure 3. (a) Mixed mode behavior of cohesive element for glass/epoxy and carbon/epoxy composite. (b) Bilinear cohesive zone law for glass/epoxy composite. (c) Exponential cohesive zone law for glass/epoxy composite.

The traction-separation law defines the cohesive zone behavior [74, 78]. Cohesive zone elements develop the debonding at the fiber-matrix interface based on traction – separation data [78]. Fig. 3(a) represents the cohesive zone law in Mode I and II fracture behavior [74] for composite materials. The initial behavior records high stiffness and to evaluate initiation of damage Equation (1) was used.

t_n , t_s and t_t are tractions in normal and shear direction respectively

δ_n , δ_s , δ_t are respective separations in normal and shear direction

t_n^0 , t_s^0 and t_t^0 are pure threshold values of stress in normal and shear directions.

$$\left\{ \frac{t_n}{t_n^0} \right\}^2 + \left\{ \frac{t_s}{t_s^0} \right\}^2 + \left\{ \frac{t_t}{t_t^0} \right\}^2 = 1 \quad (1)$$

G_n , G_s , G_t are energy used by the traction in normal and shear directions

G_n^c , G_s^c , G_t^c are threshold energy used by the traction for failure in normal and shear directions

$$G_n^c + (G_s^c - G_n^c) \left\{ \frac{G_s}{G_T} \right\} = G^c \quad (2)$$

$$G_s = G_s^c + G_t^c, \quad G_T = G_n^c + G_s^c$$

$$D = \frac{\delta_m^f (\delta_m^{\max} - \delta_m^o)}{\delta_m^{\max} (\delta_m^f - \delta_m^o)} \quad (3)$$

$$\delta_m^f = \frac{2G^c}{T_{eff}^o} \quad (4)$$

The area under traction-separation curve is equal to the fracture energy which is considered as damage evolution. For exponential traction-separation behavior in composites, the mixed mode behavior as shown in Equation (2) is used. The Equations (3) and (4) are used for calculating the damage evolution which is used for traction separation behavior for brain material. Fig. 4 shows the constitutive law of cohesive elements [74] for brain material that has been used in this study. In the above equation (3) and (4), T_{eff}^o is the effective traction at damage initiation and δ_m^{\max} refers to the maximum value of the effective displacement attained during the loading history (Figure 4).

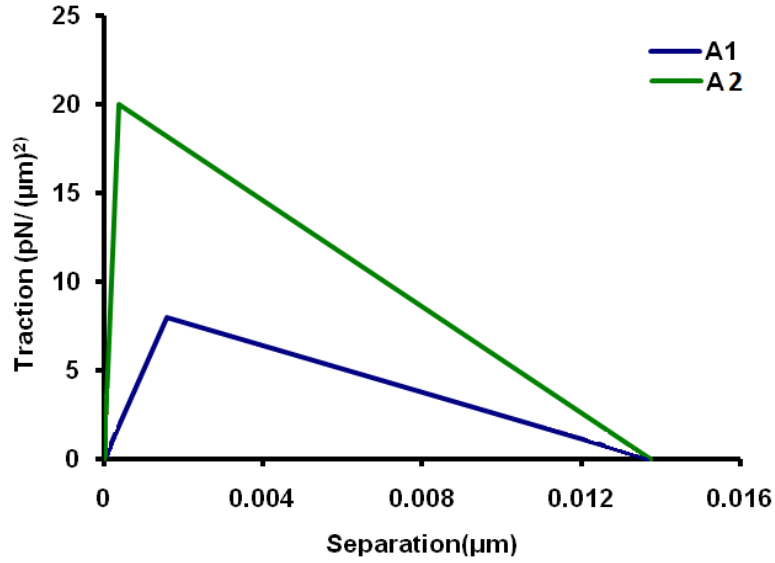


Figure 4. Independent mode bilinear behavior of cohesive element for axon-ECM composite with three different traction-separation data.

3.5 Loading and Periodicity Constraints

The three types of loadings for straight fiber include one axial, one compressive and one shear strain as shown in (Fig. 5). The four types of loadings for wavy fiber include two axial, one compressive and one shear strain as shown in (Fig. 5). Periodic boundary conditions are enforced for all load scenarios in order to form a repeated periodic structure. Referring to (Fig. 5), the 1, 2, and 3 directions are considered as the longitudinal along the direction of fiber, transverse perpendicular to the direction of fiber, and transverse along the direction of fiber respectively.

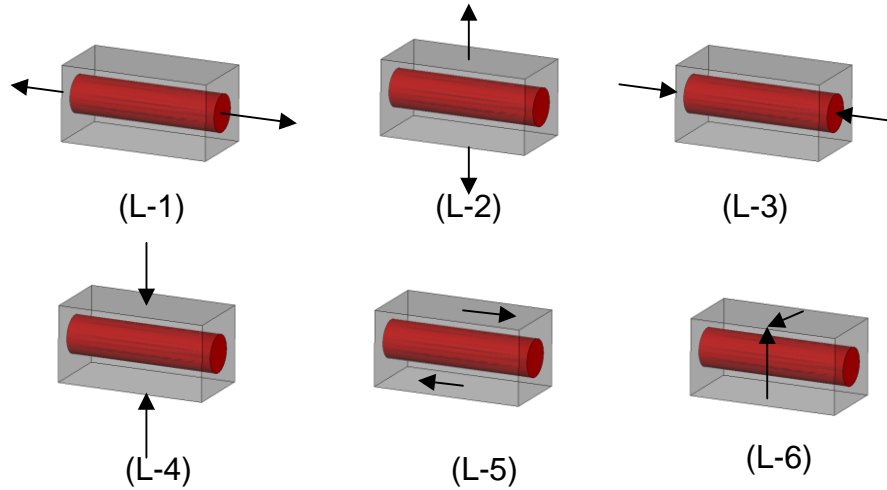


Figure 5. Schematic of the possible load scenarios.

Load Case 1 and 2: classified as when axial strain applied in direction 1 and 2 normal to faces 1 and 3 applied individually at the center node of surfaces 1 and 3 correspondingly. The load scenarios develop micro stresses and strains associated with uniform uniaxial normal stress σ_{11} and σ_{22} as in tensile direction.

Load Case 3 and 4: classified as when compressive strain applied opposite to direction 1 and 2 and normal to faces 1 and 3 enforced individually at the node located at the middle of surfaces 1 and 3 respectively. The load scenarios develop micro stresses and strains associated with uniform uniaxial stress σ_{11} and σ_{22} as in compressive direction.

Load Case 5: classified as when strain in 1-direction on the face 3 and is subjected on the center-node of face 3. This loading scenario develops micro stresses and strains associated with uniform longitudinal shear stress σ_{12} in a lamina.

3.6 *Periodicity and Rigid Body Motion Constraints*

Periodicity is achieved when opposite faces of the RUC misshape in the same fashion. Also, some constraint relations are enforced among the nodes on the faces. In order to invoke the defined constraints, the count and nodes on opposite faces of the RUC should be identical. On each surface, a node is picked at the geometrical center where loading is applied in certain load scenarios [64, 65, 94]. In order to stop rigid motion, the central node of the RUC is restricted to move in all directions. In order to stop rotations and translations, the center nodes on surfaces 1 and 2 are restricted to move in directions 2 and 3. Also, on one of the edges of face 1 a node is constrained in 2 or 3 direction based on the edge chosen in order to stop rigid rotation along the length of the unit cell.

CHAPTER 4. MICROMECHANICAL EVALAUTION OF MATERIAL DEGRADATION OF FIBROUS COMPOSITES DUE TO INTERFACIAL FAILURE

4.1 Introduction

In order to study the degradation of mechanical response of composite materials, the unit cell is applied with total of five load scenarios in which cohesive zone has a dominant role. These load cases when applied, will produce six different sets of stress and strain values. From the above stress strain values, the compliance or stiffness matrix can be calculated using the elasticity relations. For anisotropic materials, the stiffness matrix is fully populated which can be written as below.

$$\begin{Bmatrix} \epsilon_{11} \\ \epsilon_{22} \\ \epsilon_{33} \\ \epsilon_{12} \\ \epsilon_{13} \\ \epsilon_{23} \end{Bmatrix} = \begin{bmatrix} S_{1111} & S_{1122} & S_{1133} & S_{1112} & S_{1113} & S_{1123} \\ S_{2211} & S_{2222} & S_{2233} & S_{2212} & S_{2213} & S_{2223} \\ S_{3311} & S_{3322} & S_{3333} & S_{3312} & S_{3313} & S_{3323} \\ S_{1211} & S_{1222} & S_{1233} & S_{1212} & S_{1213} & S_{1223} \\ S_{1311} & S_{1322} & S_{1333} & S_{1312} & S_{1313} & S_{1323} \\ S_{2311} & S_{2322} & S_{2333} & S_{2312} & S_{2313} & S_{2323} \end{bmatrix} \begin{Bmatrix} \sigma_{11} \\ \sigma_{22} \\ \sigma_{33} \\ \tau_{12} \\ \tau_{13} \\ \tau_{23} \end{Bmatrix} \quad (5)$$

where S_{ijkl} are elements of 6×6 matrix of stiffness coefficients for a pure anisotropic material which has 21 independent coefficients. As mentioned earlier, the RUC of the composite will be subjected to five independent loading scenarios as cohesive zone is dominant in these load cases and the degradation of material properties is studied eventually from the respective stress-strain curves.

Volume averaged stresses and strains are captured from the analysis for each of the load scenarios over the volume of the RUC, i.e.,

$$\bar{\sigma}_{ij} = \frac{1}{V} \int_V \sigma_{ij} dV, \quad \bar{\varepsilon}_{ij} = \frac{1}{V} \int_V \varepsilon_{ij} dV \quad (6)$$

‘V’ represents the volume of the unit cell

4.2 *Material Input of Adhesion and Constituents*

Two different fiber-matrix constitutive material sets for two different geometries with two different mixed mode traction-separation data [86, 95] are considered for this study. The composite #1 is an epoxy matrix embedded with glass fiber which is used as material input for wavy geometry, whereas composite #2 contains carbon fibers reinforced in epoxy matrix which is used as material input for unidirectional straight fiber geometry. The materials chosen for composite #1 are isotropic where as for transverse isotropic behavior, carbon fibers are considered in composite # 2. The mechanical behavior of the composite constituents and interface parameters are included in Tables (1, 2 and 3). The behavior of composite can be evaluated as isotropic to anisotropic which is based on the constitutive materials and adhesion. The micromechanical model will determine the isotropic behavior based on the number of independent constants. The algorithm has also been implemented for unidirectional glass/epoxy composite with mode independent bi-linear and exponential cohesive zone behavior so as study the difference in composite response with two different softening laws. To study the impact of waviness on the overall composite behavior, the algorithm has also been implemented with glass/epoxy material input for three different waviness using mode independent bi-linear cohesive zone behavior.

Table 1. Mechanical properties of the fiber and matrix [42]

	Constituent	<i>E, G (GPa)</i>	<i>V</i>
Composite #1	E-Glass fiber	72.9	0.22
	Epoxy matrix	4.5	0.45
Composite #2	Carbon fiber	$E_1=201.0, E_2=E_3=13.5,$ $G_{12}=G_{13}=95, G_{23}=4.9$	$\nu_{12}=\nu_{13}= 0.22$ and $\nu_{23}=0.25$
	Epoxy matrix	4.5	0.45

Table 2. Mechanical properties of interface elements for Composite #1 [41]

Elastic Properties $K_{nn} = K_{ss} = K_{tt}$	$3.0687 \times 10^4 \text{ N/mm}^3$
Max Nominal Stress $N_0 = T_0 = S_0$	40 MPa
Fracture Energy, G_{IC} $G_{IIC} = G_{IIIC}$	0.25 N/mm, 1.08 N/mm

Table 3. Mechanical properties of interface elements for Composite #2 [40]

Elastic Properties $K_{nn} = K_{ss} = K_{tt}$	$2.01 \times 10^4 \text{ N/mm}^3$
Max Nominal Stress $N_0 = T_0 = S_0$	36.3 MPa
Fracture Energy, G_{IC} $G_{IIC} = G_{IIIC}$	0.0075 N/mm, 0.6 N/mm

CHAPTER 5. COMPARISON OF MICROMECHANICAL MATERIAL DEGRADATION OF UNIT CELLS WITH DIFFERENT ADHESION BEHAVIOR AND UNDULATIONS

5.1 Material Degradation of Unidirectional Carbon/Epoxy Composite with Mixed Mode- Bilinear Traction Separation Based Cohesive Zone

To represent adhesion between fiber and matrix in composite, hexagonal unit cell is created (Fig. 1(a)). The unidirectional carbon/epoxy composite with hexagonal packing is subjected to three different load cases which comprises of tensile loading in 2-2 direction (Load Case-2), compressive loading in 2-2 direction (Load Case-4) and shear loading in 1-2 direction (Load Case-5). These load cases represent almost all possible load scenarios in the real world of composite application in which cohesive zone has a dominant role. The majority of cohesive zone approaches is focused on single mode loading and generally is performed under mode-I loading scenario. It is unfortunate that single-mode loading hardly occurs in practice and in most cases the energy dissipated in Mode-I and Mode-II are not equal. In mixed-mode loading, decohesion or separation is not linear but instead drives away from its actual direction. Also, at micro scale level, because of the microstructural features (e.g. grain size, adhesion size and shape) such variations in decohesion direction may occur even under pure mode-I loading case. Mixed Mode cohesive zone behavior has been implemented to study the overall composite response. Volume average stresses and strains are considered to study the effect of cohesive zone on the overall composite behavior. The hexagonal RVE subjected

to tensile loading (L-2) shows a rapid material degradation of composite at a strain of 0.006 and with increasing displacement the interface undergoes decohesion as shown in Fig. 6. The stiffness neutralizes at a strain of 0.012 when the interface separates completely. In this load case the composite attains a maximum stress of 40.8MPa and then the material starts to degrade and is continued by a steady stiffness region leading to a locked phase.

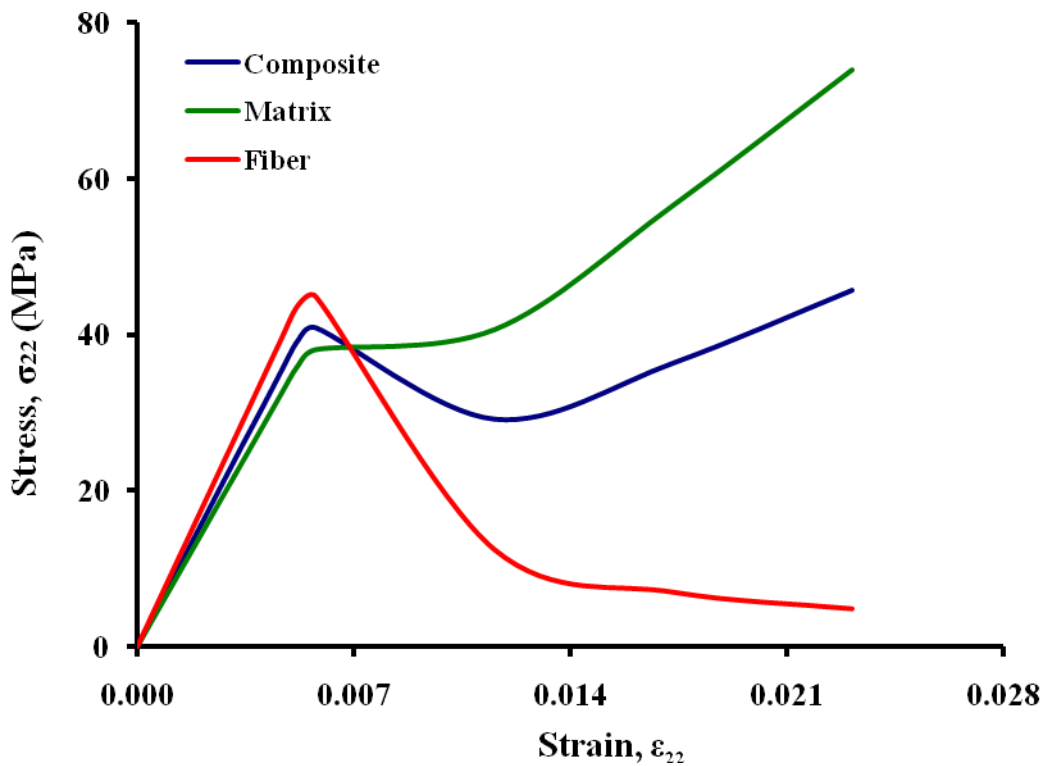


Figure 6. Tensile stress-strain distribution in fiber, matrix, and composite due to the applied strain in direction 2-2 in a unidirectional carbon/epoxy composite model of $V_F/V=0.4$.

From Fig. 6, one interesting observation that can be found is that in the stress-strain plot, there exists a point where all the three constituent's (fiber, matrix and composite) stresses

are equal and we can infer that till this point fiber is the major load carrier and after this point stresses in fiber relax and matrix becomes the major load carrier.

Similar formats are observed for the shear and compressive loadings (Figs. 7 and 8). In shear load case, the maximum stress attained by the composite is 30MPa but for compressive loading the initiation of degradation occurs at a peak stress of 87.5MPa which is nearly twice when compared to the maximum stress attained by the composite for tensile loading (L-2). From Fig (7 and 8), for the same strain of 0.012, the composite in shear and compressive loading starts to degrade and we can infer that composite in compressive loading is vulnerable. For all the load cases, the composite reaches a peak stress and then degrades and is followed by a constant stiffness. Similar trend of composite behavior has also been observed in Inglis et.al (2005) with cohesive zone model using numerical simulations [79].

The tensile, compressive and shear strength evaluated by using this micromechanics tool are 40.8MPa, 87.5MPa and 32MPa respectively and the initial stiffness evaluated for tensile, compressive and shear loading are 7.1GPa, 7.13GPa and 3.5GPa respectively. The strength and initial stiffness of composite material for all the load cases evaluated using this micromechanics tool are comparable with the published results for carbon/epoxy composites [78, 80-84] The difference in the numerical values of evaluated strength and stiffness when compared to published results is because of the factors like volume fraction, fiber packing and fiber sizing (see Table 4).

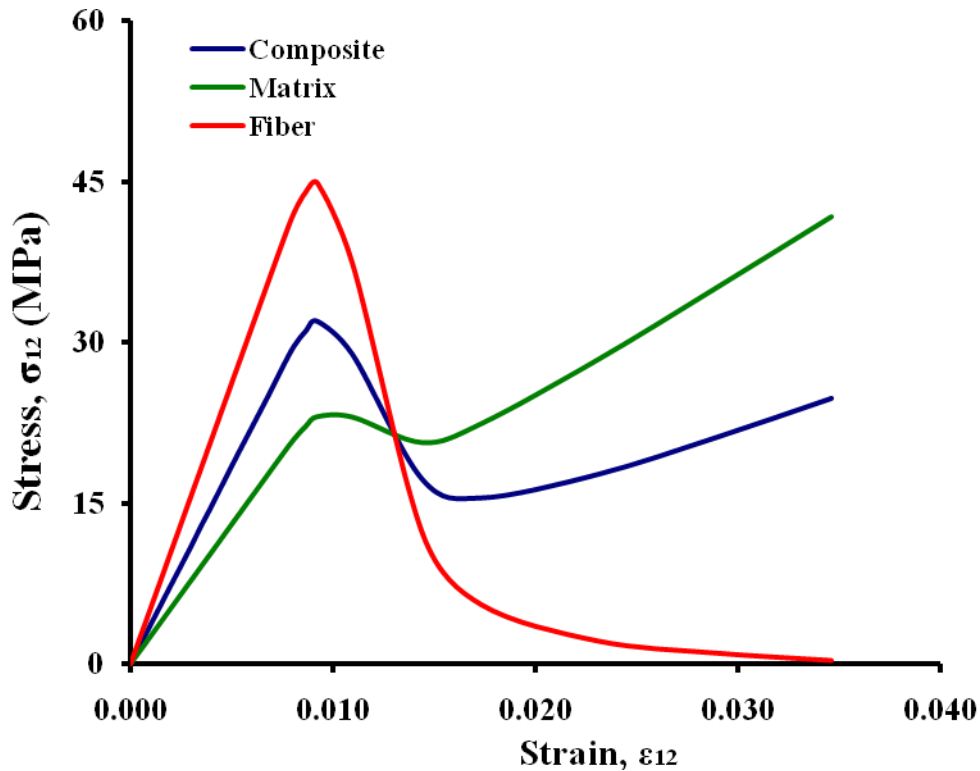


Figure 7. Shear stress-strain distribution in fiber, matrix, and composite due to the applied strain in direction 1-2 in a unidirectional carbon/epoxy composite model of $V_F/V=0.4$.

5.2 Material Degradation of Wavy Glass/Epoxy Composite with Mixed Mode-Bilinear Traction Separation Based Cohesive Zone

To represent adhesion between fiber and matrix in composite, hexagonal wavy model is created. As discussed earlier, in fabrication of composites, flaws such as the undulation of fibers that develop during filament winding process or other fabrication processes produce variable mechanical properties when compared to straight fiber composites and that is reason to implement the wavy model (Fig. 1(b)). The wavy model implemented for this study is of amplitude/wavelength (A/L) of 0.085. The wavy glass/epoxy composite with hexagonal packing is subjected to four different load cases

which comprises of tensile loading in 1-1 direction (Load Case-1), compressive loading in 1-1 direction (Load Case-3), tensile loading in 2-2 direction (Load Case-2) and shear loading in 1-2 direction (Load Case-5). These load cases represent almost all possible load scenarios in the real world of wavy composite application in which cohesive zone has a dominant role. In composite unit cell with unidirectional fiber model, loading in longitudinal direction (Load case-1) did not have any significant impact on the overall

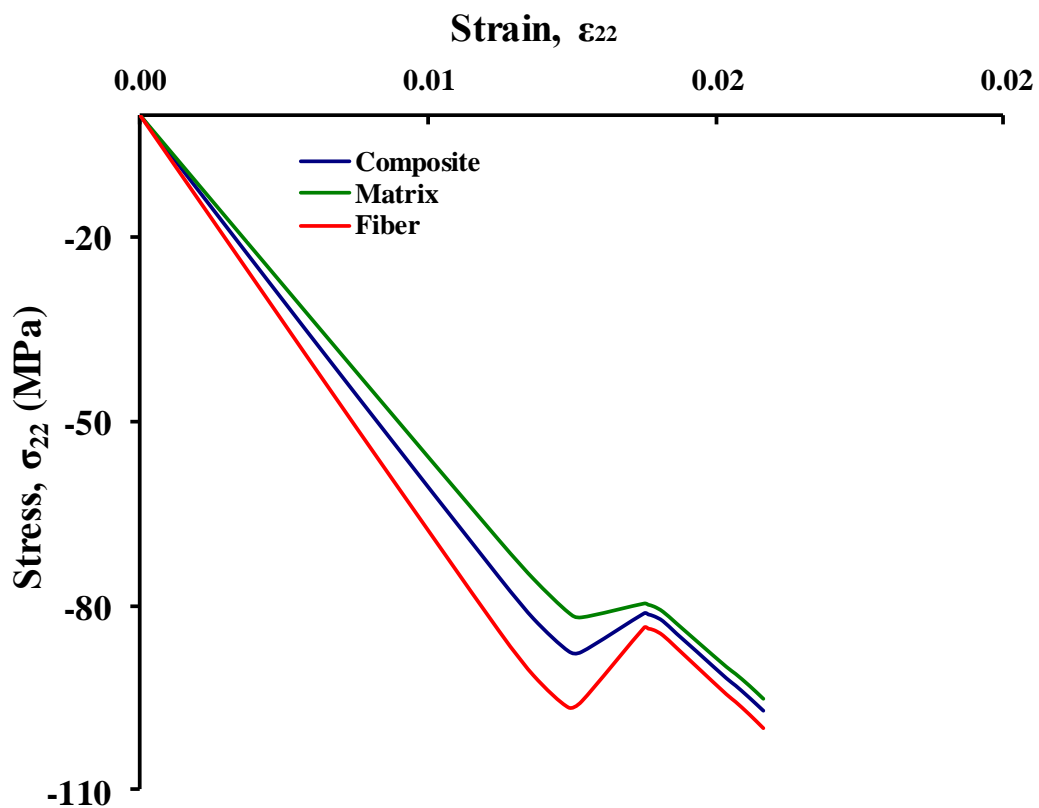


Figure 8. Compressive stress-strain distribution in fiber, matrix, and composite due to the applied strain in direction 2-2 in a unidirectional carbon/epoxy composite model of $V_F/V=0.4$.

Table 4. Comparison of initial stiffness and strength of unidirectional carbon/epoxy composite calculated using the proposed method with the available literature data

Mechanical Properties:-	Proposed Method	Literature[40,44-48]
Tensile Strength-Transverse	40.8MPa	40-60MPa
Compressive Strength-Transverse	87.5MPa	50-250MPa
Shear Strength	32MPa	25-50MPa
Young's Modulus- Transverse	7.1GPa	7-10GPa
Shear Modulus	3.5GPa	3.3-5.2GPa
Volume fraction	40%	30-60

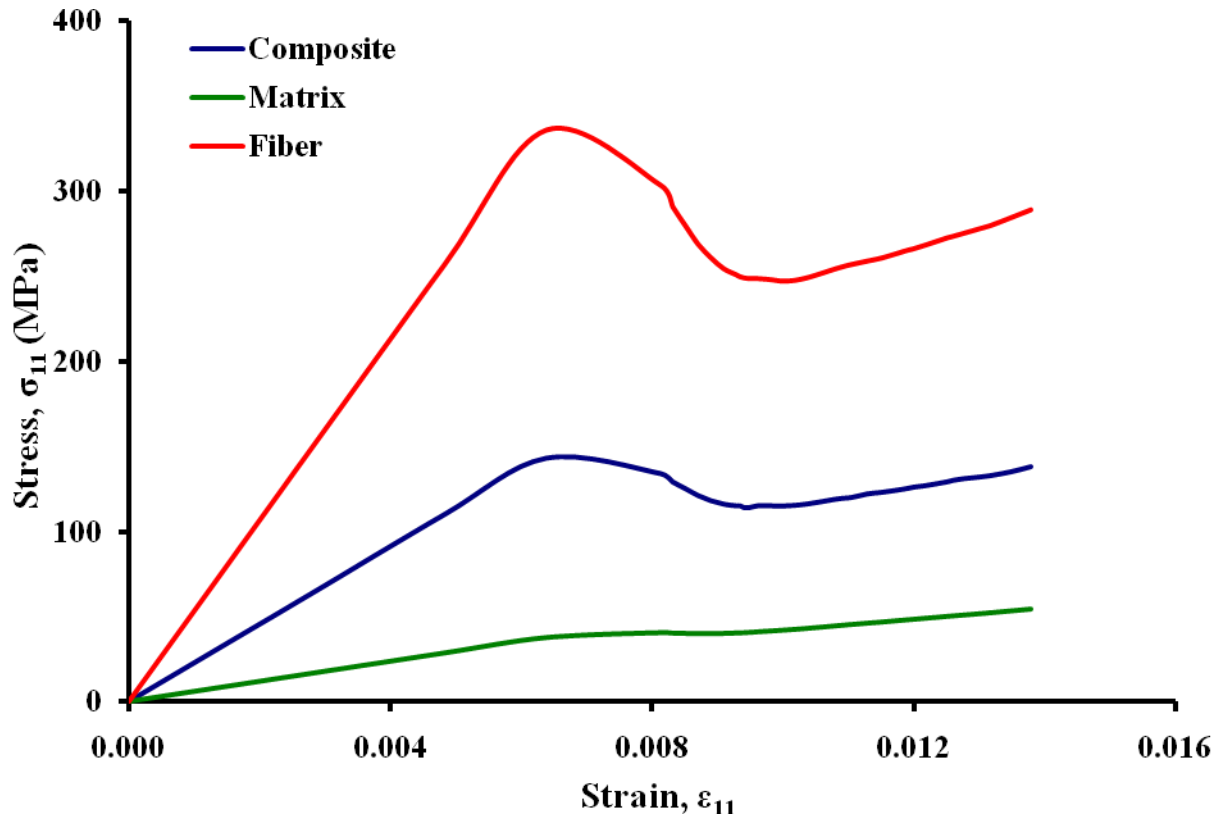


Figure 9. Tensile stress-strain distribution in fiber, matrix, and composite due to the applied strain in direction 1-1 in a glass/epoxy composite model with waviness ($A/L=0.085$) of $V_F/V=0.4$.

stress distribution in fiber or matrix. However, for wavy models both fiber and matrix have an impact due to longitudinal loadings. Since in wavy models, fibers are oriented over a curvature in a local direction, the global stresses should not remain constant.

Mixed Mode cohesive zone behavior has been implemented to study the overall composite response. The hexagonal packed wavy model subjected to longitudinal loading also shows a rapid material degradation of wavy composite at a strain of 0.0064 and with increasing displacement the adhesion area undergoes debonding as shown in Fig. 9. The stiffness of wavy composite neutralizes at a strain of 0.0096 when the interface region separates completely. In this load case, the wavy composite reaches a maximum stress of 143MPa and then the material starts to degrade and is followed by a constant stiffness phase. From Fig. 11, for compressive loading in the same direction 1-1, the wavy composite reaches a peak stress of 185MPa at a strain of 0.0087, which infers that the wavy composite has more compressive strength in 1-1 direction when compared to longitudinal strength. Similar trends are seen for the tensile (L-2) and shear (L-5) loading (Figs. 10 and 12) as seen for unidirectional unit cell model. From the Figs. 10 and 12, one interesting observation that can be found is that in the stress-strain plots, wavy composite has more or less the same peak stress but with significant different strains which infers that the wavy composite has more tensile strength in 2-2 direction when compared to shear strength in the same direction.

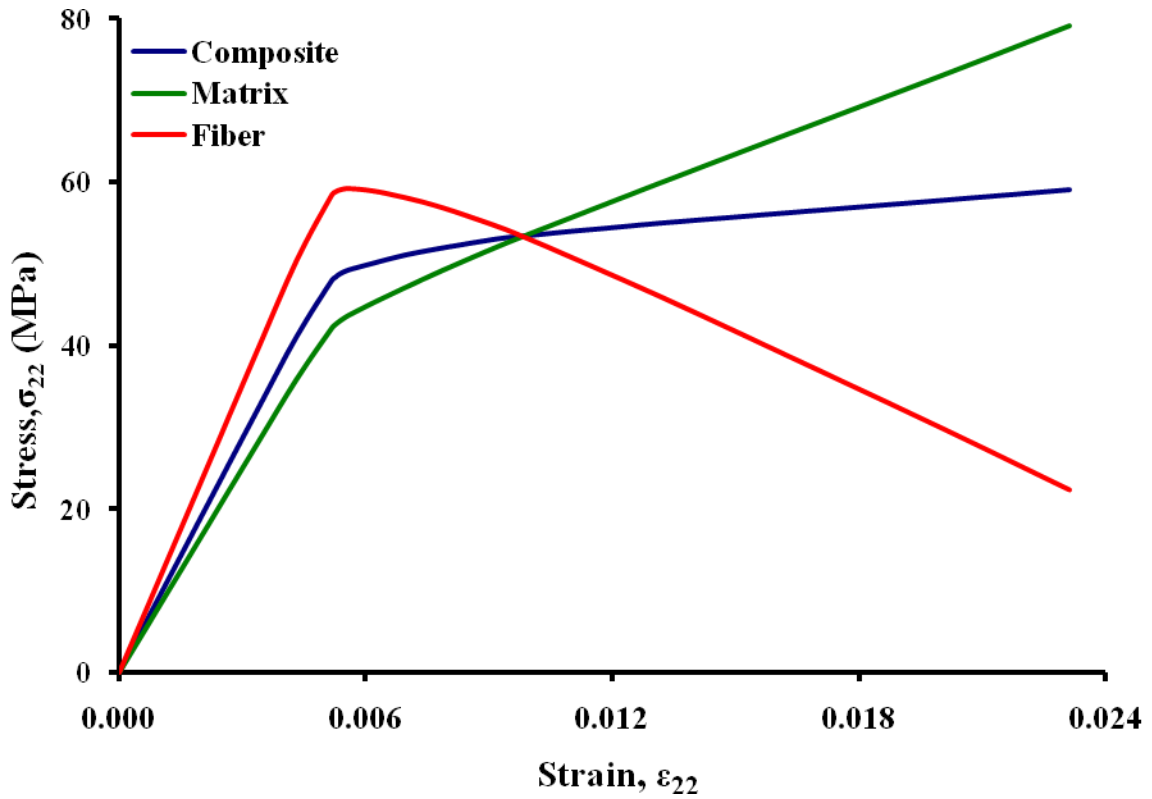


Figure 10. Tensile stress-strain distribution in fiber, matrix, and composite due to the applied strain in direction 2-2 in a glass/epoxy composite model with waviness ($A/L=0.085$) of $V_F/V=0.4$.

5.3 Comparison of Material Degradation of Unidirectional Glass/Epoxy Composite

Using Bilinear and Exponential Traction Separation Cohesive Zone Laws

In this study, we have implemented exponential cohesive zone law for unidirectional glass/epoxy composites and the difference between bi-linear and exponential cohesive zone law on the overall composite behavior has been studied. The strength of the composite is based on the fiber sizing techniques and the type of manufacturing process employed. On this basis, specific shape of the cohesive zone law can be implemented to determine the experimental strength of the composite in all the directions. The unidirectional hexagonal packed glass/epoxy composite is subjected to

same load cases as discussed in section 4.1. For the ease of calculations and faster convergence, we have implemented single mode cohesive zone behavior in this study [74]. In this study, we have assumed same fracture energy and same peak stress in the cohesive zone but with different softening laws (Fig 3). We observed a significant difference by comparing the stress-strain plots of unidirectional glass/epoxy composite when subjected to load cases (L-2, L-4 and L5) using bi-linear and exponential traction-separation cohesive zone laws. For the entire load cases, from the Figs. 13, 14 and 15, the initial stiffness for the composite remains the same and then the material starts to degrade

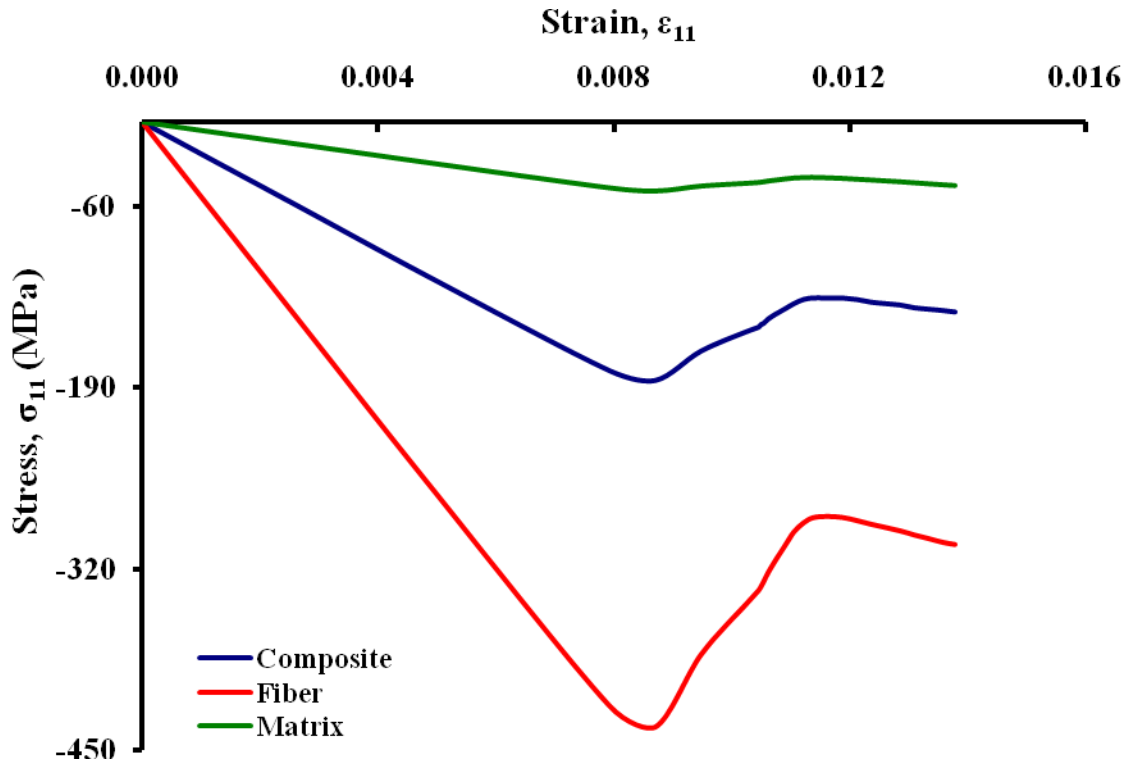


Figure 11. Compressive stress-strain distribution in fiber, matrix, and composite due to the applied strain in direction 1-1 in a glass/epoxy composite model with waviness ($A/L=0.085$) of $V_F/V=0.4$.

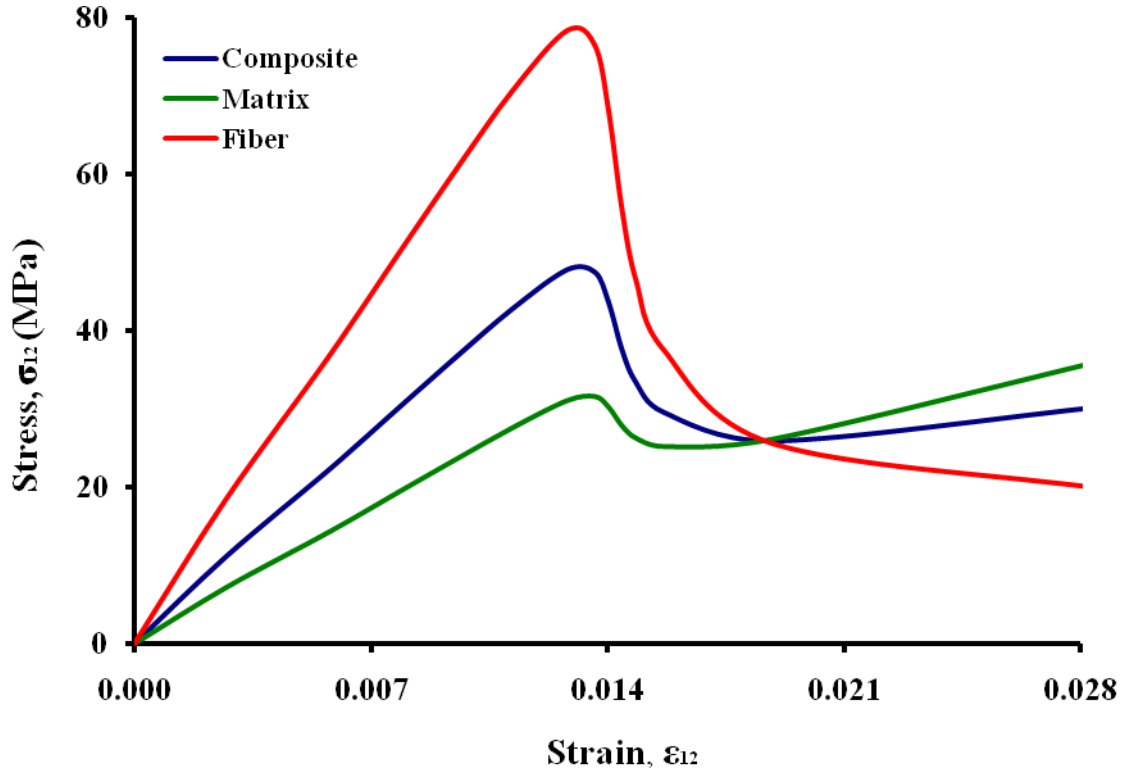


Figure 12. Shear stress-strain distribution in fiber, matrix, and composite due to the applied strain in direction 1-2 in a glass/epoxy composite model with waviness ($A/L=0.085$) of $V_F/V=0.4$.

and is followed by a constant stiffness. The major difference observed while implementing the bi-linear and exponential traction-separation cohesive zone laws is that the peak stress attained by the composite has shifted more than twice in the case of exponential cohesive zone law. From this result, for all the load cases we can infer that the unidirectional composite when implemented with exponential cohesive zone law has more strength in all the directions when compared to the composite implemented with bi-linear cohesive zone law. Based on the stress-strain plots of the composite from the experimental results, proper cohesive zone law can be determined. For all the load cases, we have also observed that the response of the unidirectional composite when

implemented with both the cohesive zone laws, stabilizes with same stiffness after the interface debonds completely.

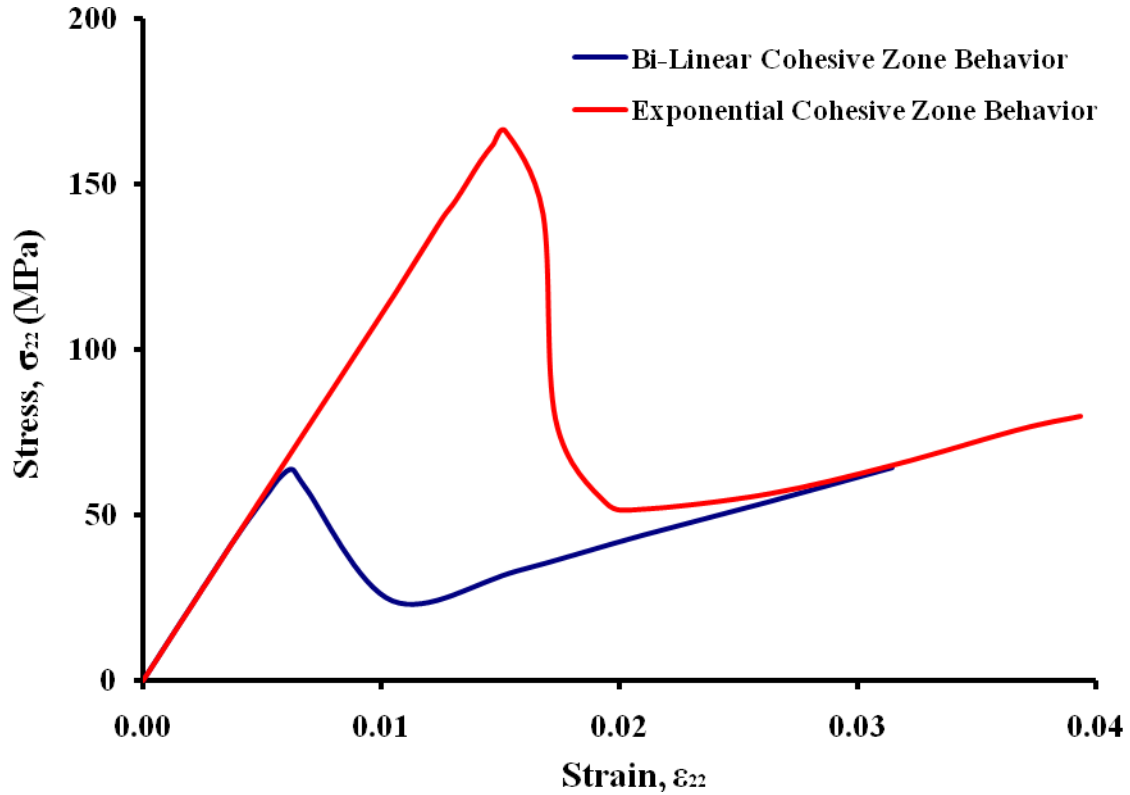


Figure 13. Tensile stress-strain distribution in unidirectional glass/epoxy composite models of $V_F/V=0.4$ due to the applied strain in direction 2-2 with two different (bilinear and exponential) traction-separation behaviors.

5.4 Comparison of Material Degradation of Glass/Epoxy Composite with Different Waviness of Fiber

As discussed earlier, due to defects in fabrication process of composites, undulation of fibers may occur. In this study, we would like to concentrate the effect of waviness or undulation on the overall composite behavior using cohesive zone method. The wavy models implemented for this study are of amplitude/wavelength (A/L) of

0.085, 0.121 and 0.179. The hexagonal packed glass/epoxy composite with three different undulations are subjected to same load cases as discussed in section 3.5. For the ease of calculations and faster convergence, we have implemented single mode bilinear cohesive zone behavior in this study [74]. From the Fig. 17, the wavy models with different waviness when subjected to longitudinal loading (L-1) had a significant impact on the initial stiffness and longitudinal strength of composite. It can be observed that, with increase in waviness, the initial stiffness and peak stress attained by composite decreases. It is also observed that waviness has no big impact on the composite behavior

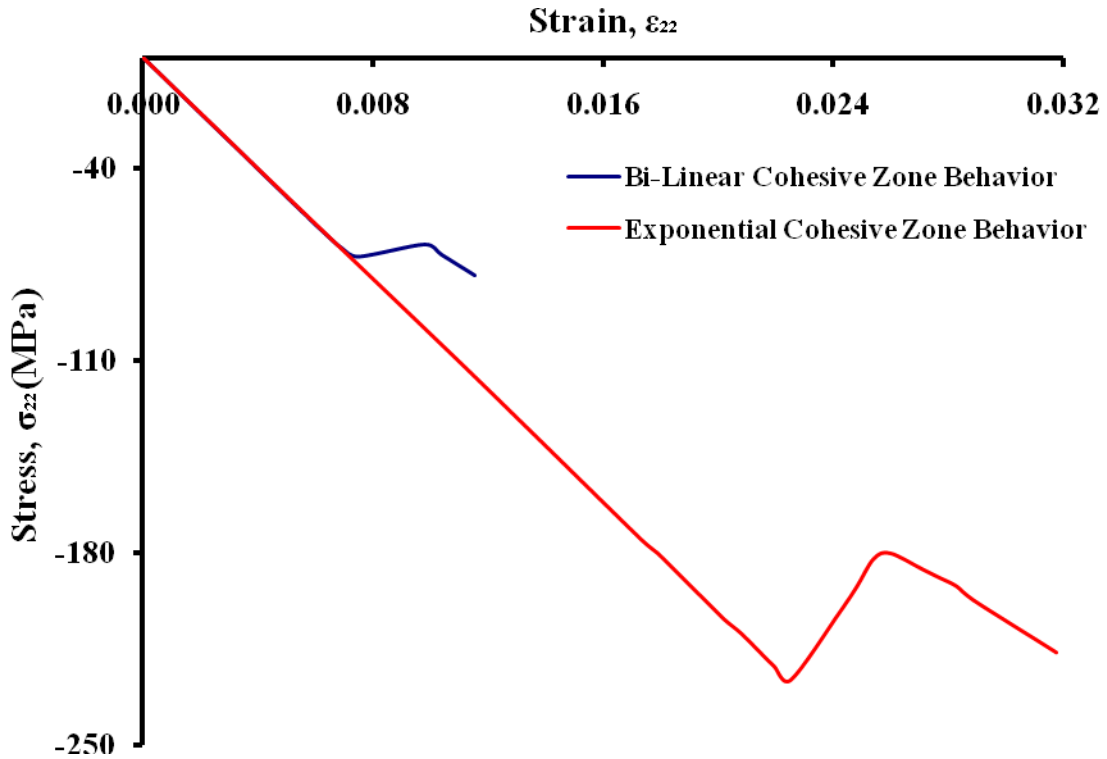


Figure 14. Compressive stress-strain distribution in unidirectional glass/epoxy composite models of $V_F/V=0.4$ due to the applied strain in direction 2-2 with two different (bilinear and exponential) traction-separation behaviors.

after the interface has debonded completely. Similar trend is also observed when the composite with increasing waviness is subjected to compressive loading (L-3) in 1-1 direction. From fig. (17), when the composites with increasing waviness is subjected to transverse loading in 2-2 direction, similar trend is observed as discussed for longitudinal loading but the difference due to waviness is not that significant when compared with longitudinal and compressive loading in 1-1 direction. As discussed in section 4.1, from fig. (16 and 18), it is observed that wavy composites have more compressive strength in 1-1 direction when compared to longitudinal strength in the same direction. This means that the introduction of more wavy fibers will decrease the overall composite stiffness and strength in longitudinal compression and transverse directions. However, from

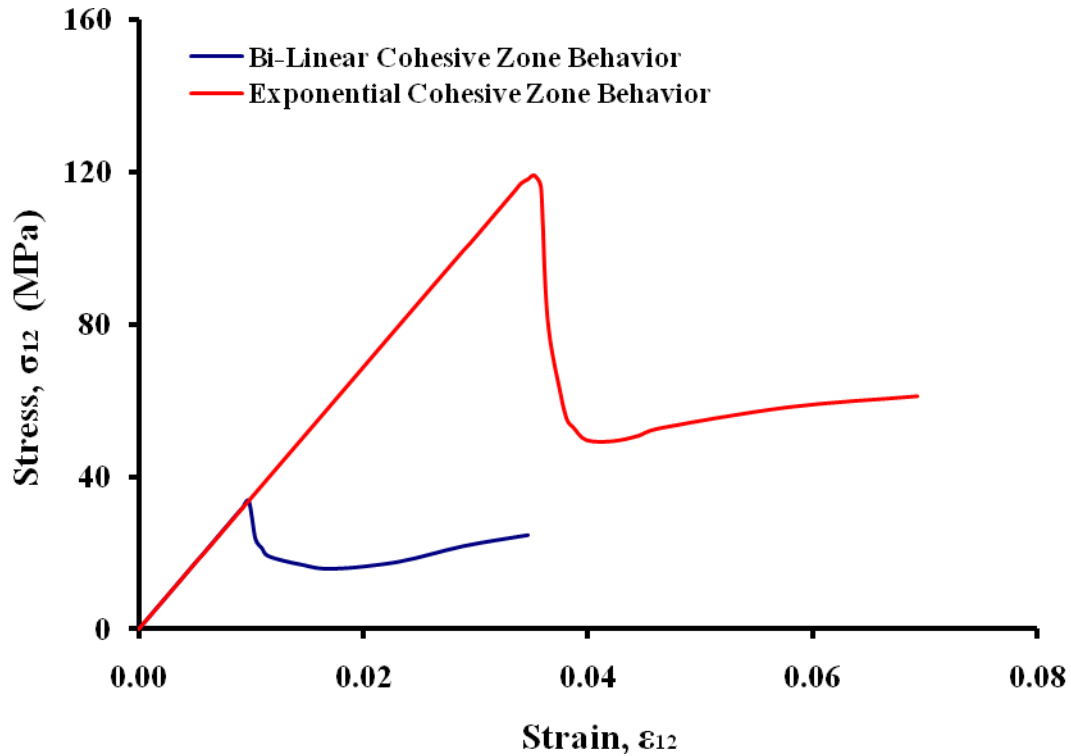


Figure 15. Shear stress-strain distribution in unidirectional glass/epoxy composite models of $V_F/V=0.4$ due to the applied strain in direction 1-2 with two different (bilinear and exponential) traction-separation behaviors.

fig.(19) when composites with increasing waviness is subjected to shear loading (L-5), it can be observed that with increase in waviness, the initial stiffness and peak stress attained by composite increases. Hence composite materials with more wavy fiber distribution will result in a stronger material for shear.

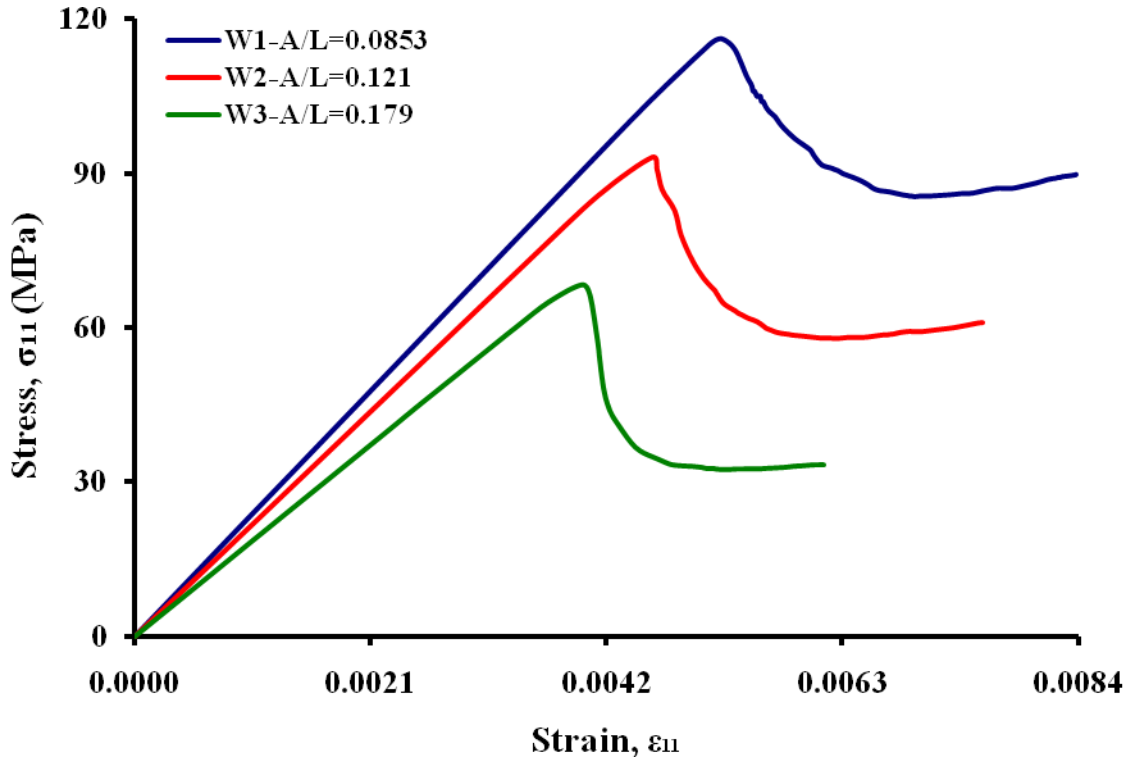


Figure 16. Tensile stress-strain distribution in glass/epoxy composite models of $V_F/V=0.4$ due to the applied strain in direction 1-1 for three different waviness ($A/L=0.0853$, 0.121 , 0.179).

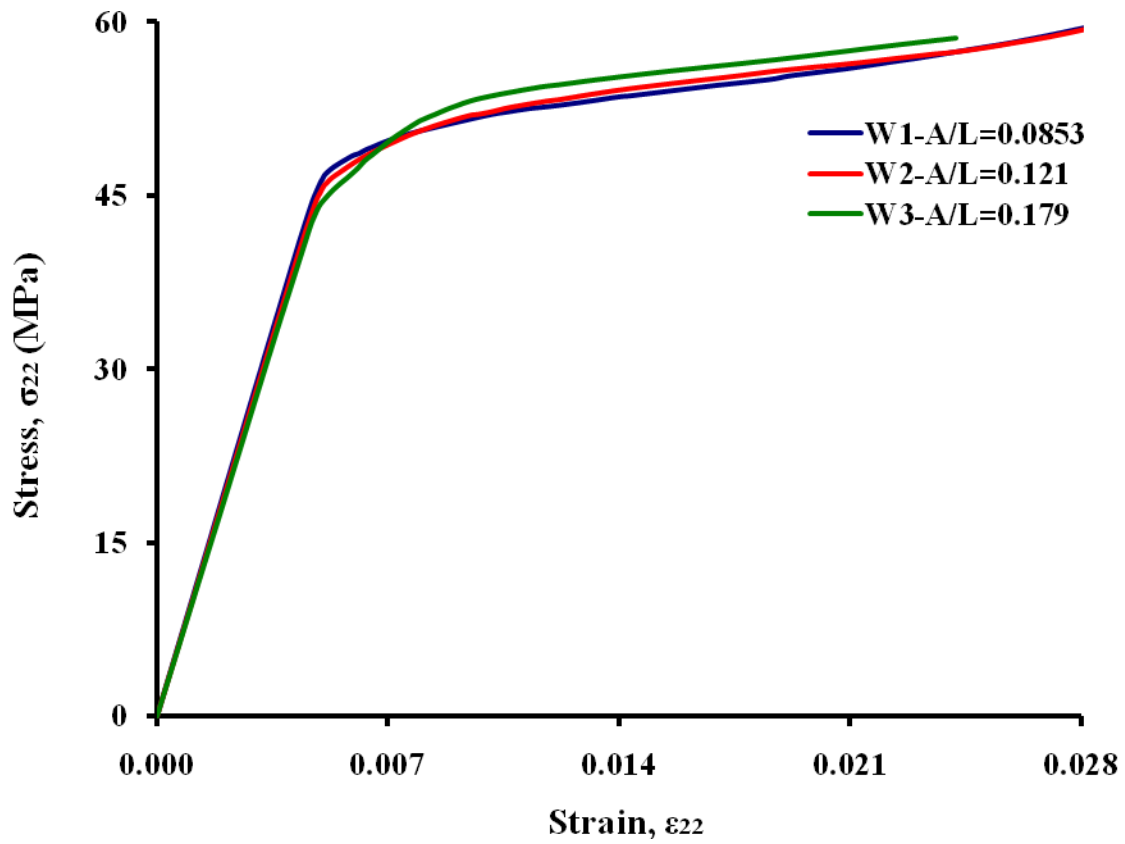


Figure 17. Tensile stress-strain distribution in glass/epoxy composite models of $V_F/V=0.4$ due to the applied strain in direction 2-2 for four different waviness ($A/L=0, 0.0853, 0.121, 0.179$).

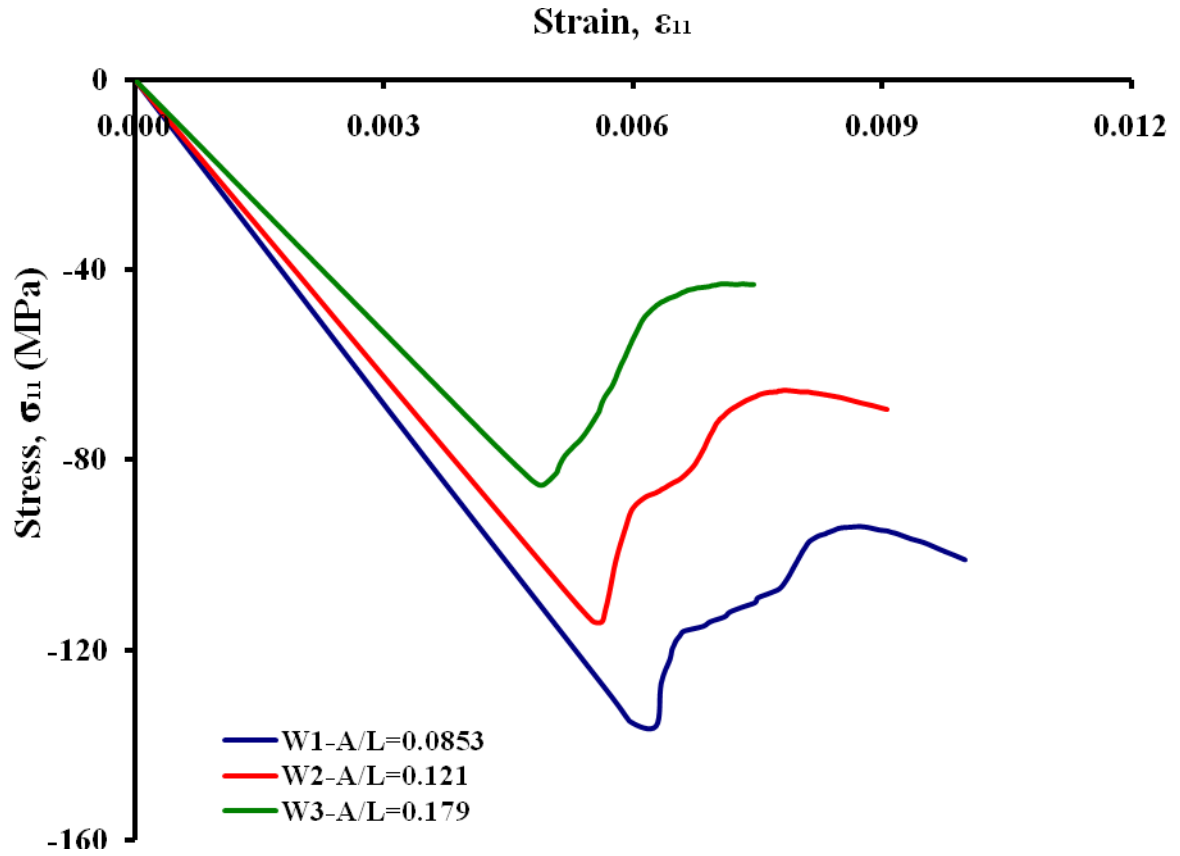


Figure 18. Compressive stress-strain distribution in glass/epoxy composite models of $V_F/V=0.4$ due to the applied strain in direction 1-1 for three different waviness ($A/L=0.0853, 0.121, 0.179$).

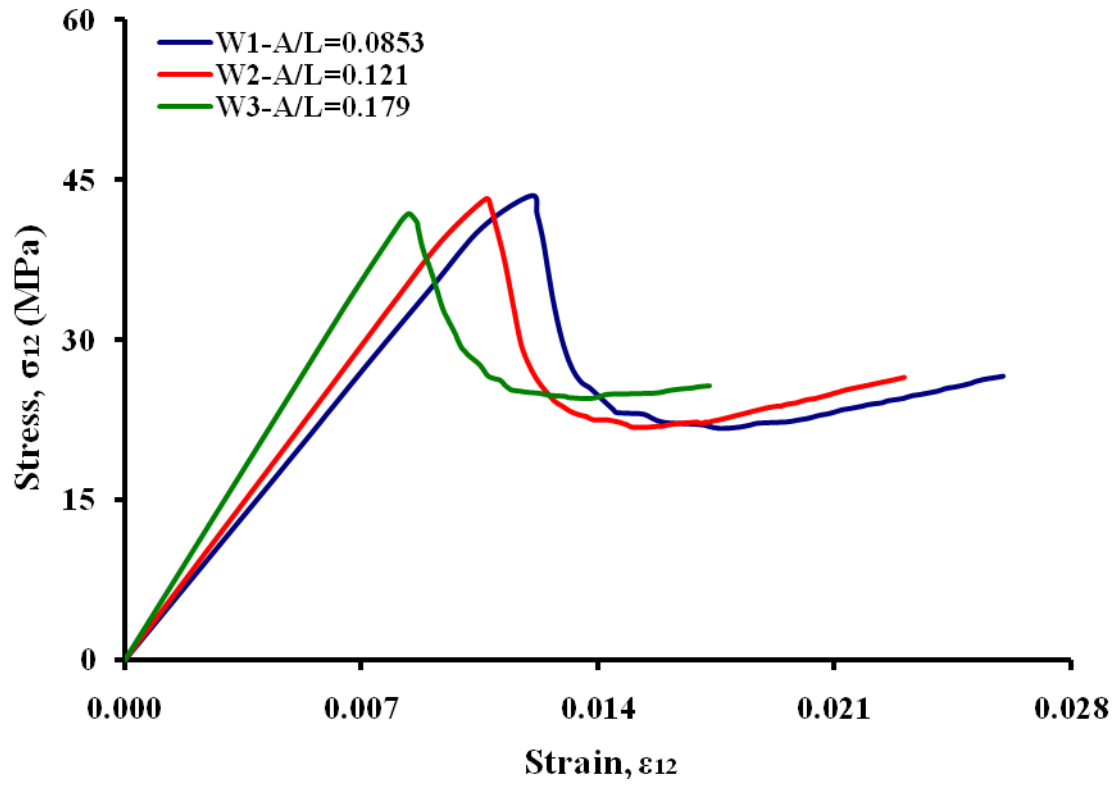


Figure 19. Shear stress-strain distribution in glass/epoxy composite models of $V_F/V=0.4$ due to the applied strain in direction 1-2 for four different waviness ($A/L=0, 0.0853, 0.121, 0.179$).

CHAPTER 6. EFFECT OF ADHESION ON VISCOELASTIC CHARACTERIZATION OF MECHANICAL PROPERTIES OF BRAIN WHITE MATTER

6.1 Introduction

Brain material response is dependent on loading scenarios, strain gradients, temperature and some physical parameters on a continuum level. The response of brain material can be simulated with a variety of constitutive material models [85-90]. The material models include elastic, viscoelastic and hyperelastic behaviors. The material property of any composite can be estimated from micromechanics principles with defined properties of the constituents, fiber orientation and distribution. The material constituents implemented in our study are presumed to follow a linear viscoelastic behavior. Under small deformation cases, such material assumptions are widely accepted. The linear viscoelastic behavior under small deformation assumption is evaluated as below.

$$\sigma_{ij}(t) = \int_0^t C_{ijkl}(t-\tau) \frac{d\varepsilon_{kl}(\tau)}{d\tau} d\tau, \quad i, j, k, l = 1, 2, 3 \quad (7)$$

The above stress-strain can be converted into Voigt vector form as:

$$\begin{Bmatrix} \sigma_{11}(t) \\ \sigma_{22}(t) \\ \sigma_{33}(t) \\ \sigma_{12}(t) \\ \sigma_{13}(t) \\ \sigma_{23}(t) \end{Bmatrix} = \int_0^t \begin{bmatrix} C_{1111} & C_{1122} & C_{1133} & C_{1112} & C_{1113} & C_{1123} \\ C_{2211} & C_{2222} & C_{2233} & C_{2212} & C_{2213} & C_{2223} \\ C_{3311} & C_{3322} & C_{3333} & C_{3312} & C_{3313} & C_{3323} \\ C_{1211} & C_{1222} & C_{1233} & C_{1212} & C_{1213} & C_{1223} \\ C_{1311} & C_{1322} & C_{1333} & C_{1312} & C_{1313} & C_{1323} \\ C_{2311} & C_{2322} & C_{2333} & C_{2312} & C_{2313} & C_{2323} \end{bmatrix} \begin{Bmatrix} d\varepsilon_{11}(\tau)/dt \\ d\varepsilon_{22}(\tau)/dt \\ d\varepsilon_{33}(\tau)/dt \\ d\varepsilon_{12}(\tau)/dt \\ d\varepsilon_{13}(\tau)/dt \\ d\varepsilon_{23}(\tau)/dt \end{Bmatrix} d\tau \quad (8)$$

The time-dependent $C_{ijkl}(t)$ is a 6×6 matrix of relaxation coefficients for a composite material and detailed explanation can be found in Abolfathi et.al [94]. Prony series expression is used with a linear viscoelastic behavior to determine the coefficients $C_{ijkl}(t)$, each with its individual sub-coefficients as [91]:

$$C_{ijkl}(t) = \bar{C}_{ijkl} \left(1 - \sum_{k=1}^n c_k (1 - e^{-t/\tau_k}) \right) \quad (9)$$

The viscoelastic behavior of a material can be characterized by determining the sub-coefficients $\bar{C}_{ijkl}, c_k, \tau_k$ associated with each coefficient $C_{ijkl}(t)$.

A detailed explanation of this micromechanical method to evaluate the viscoelastic behavior of composites is published in Garnich and Karami (2005a) and Naik et al. (2008) [92, 93]. The volume averaged stresses and strains which are time dependent are calculated from the output captured at every time step of the analysis i.e.,

$$\bar{\sigma}_{ij}(t) = \frac{1}{V} \int_v \sigma_{ij}(t) dv; \quad \bar{\varepsilon}_{ij}(t) = \frac{1}{V} \int_v \varepsilon_{ij}(t) dv \quad (10)$$

“V” represents the overall volume of the unit cell.

The stress and strain data when included in the above formulation (10) can be used as an input for calculating the 21 independent coefficients $C_{ijkl}(t)$ to represent the anisotropic behavior of the brain tissue material.

6.2 Relaxation Loading

To study the impact of adhesion of the brain tissue, the RUC of brain material is subjected to the relaxation loading. In order to study the adhesion behavior on the brain tissue with respect to time, five independent kinematical loading scenarios are

implemented (Figure 5) and the relaxation output from each load scenario is captured. The five loading scenarios are categorized as two axial displacements in 1, 2 directions and one longitudinal shear loading which represent the most possible loading scenarios in which adhesion has a dominant role. All load scenarios as a part of relaxation loading are impacted with a fixed 0.3% displacement and related data of volume average stress-strain of the overall RUC, axons and ecm are captured at every time step. The point at which the stiffness curve approaches a slope of zero is considered as end time for relaxation test. Arbogast and Margulies (1999) have reported that in brain material, the axons show more viscous behavior when compared to matrix and so the finish time of relaxation test is dependent on the axons viscoelastic behavior. In this finite element analysis, the total time duration is divided into multiple steps in order to reduce the overall computational time. At each of these defined time steps, finite element analysis is performed. The number of time intervals for this study is selected efficiently to make sure that required number of data points are captured to study the accurate effect of adhesion on the brain material.

6.3 *The Material Data for Adhesion, Axons, and Matrix*

Brain white matter is considered as a composite region of brain with multiple sub regions consisting of dissimilar geometric and mechanical behaviors. Since there is no enough constitutive material for axons and extracellular matrix, we have used the same methodology for material input of Axons and ECM as used in Abolfathi et.al [94]. The viscoelastic behavior of axons and matrix are included in Table 4.1 and 4.2. As explained earlier, the axon-ecm interface parameters have been calculated from the available bond extension data for cell adhesion [40, 52, 71].The Axon-ECM interface

parameters are presented in Table-5. The algorithm has been implemented for unidirectional Axon-ECM composite model with three different mode independent bi-linear cohesive zone behaviors so as study the difference in viscoelastic response of the brain composite model. To study the impact of waviness on the viscoelastic response of the composite behavior, the algorithm has also been implemented with three different waviness using mode independent bi-linear cohesive zone behavior.

Table 5. Viscoelastic property of axon material [63]

Instantaneous Elastic Modulus (Pa)	Poisson's Ratio	Prony Series Parameters		
63981.69	0.4999	G	k	τ
		0.895231	0	0.0103
		0.0090427	0	0.40005

* The frequency domain data available from Arbogast and Margulies (1999) converted into time domain.

Table 6. Viscoelastic behavior of ECM material

Instantaneous Elastic Modulus (Pa)	Poisson's Ratio	Prony Series Parameters		
23195.17	0.4999	g	k	τ
		0.8681981	0	0.005
		0.0437855	0	0.07995

* The frequency domain data available from Arbogast and Margulies (1999) converted into time domain.

Table 7. Mechanical properties of interface elements for the study of axon-ECM adhesion [38, 52, 71]

Elastic Properties $K_{nn} = K_{ss} = K_{tt}$ [pN/ (μm) ³]	Max Nominal Stress $N_0 = T_0 = S_0$ [pN/ (μm) ²]	Fracture Energy, $G_{IC} = G_{IIC} = G_{IIIC}$ [pN/ (μm)]
A1 5000	8	0.055
A2 20000	20	0.055

A3 is considered as 100% adhesion between fiber and matrix

CHAPTER 7. COMPARISON OF MICROMECHANICAL VISCOELASTIC BEHAVIOR OF UNIT CELLS DUE TO THE EFFECT OF DIFFERENT ADHESION AND UNDULATIONS

7.1 Impact of Adhesion on the Viscous Behavior of Axons and Matrix in a Unidirectional Brain Composite Unit Cell with Bilinear Traction Separation Based Cohesive Zone

To represent adhesion between Axon and Matrix in a brain composite model, hexagonal unit cell is created (Fig. 2(b)). The unidirectional brain composite model with hexagonal packing is subjected to three different load cases which comprises of tensile loading in 2-2 direction (Load Case-2), compressive loading in 2-2 direction (Load Case-4) and shear loading in 1-2 direction (Load Case-5). These load cases represent almost all possible load scenarios in the brain injury study in which cohesive zone has a dominant role. The majority of cohesive zone approaches is focused on single mode loading and generally is executed under mode-I loading scenario. We have also implemented all the adhesion FEM analysis under mode-I loading to reduce analysis time and to increase the speed. At micron level, based on the microstructure features, deviations in decohesion direction can also take place under pure mode-I loading case. Mode-I cohesive zone behavior has been implemented to study the impact of adhesion on the Axons, Matrix and Brain composite model. Volume average stresses and strains are considered to study the effect of adhesion on the brain unit cell model. At a constant strain of 0.03%, the hexagonal RVE when subjected to shear loading (L-4) shows the impact of different

adhesion behavior on the viscous nature of Axons, Matrix and Brain composite unit cell model. It has been observed that the stiffness and the viscous behavior of Axons, Matrix and Brain tissue is highly dependent on the adhesion property.

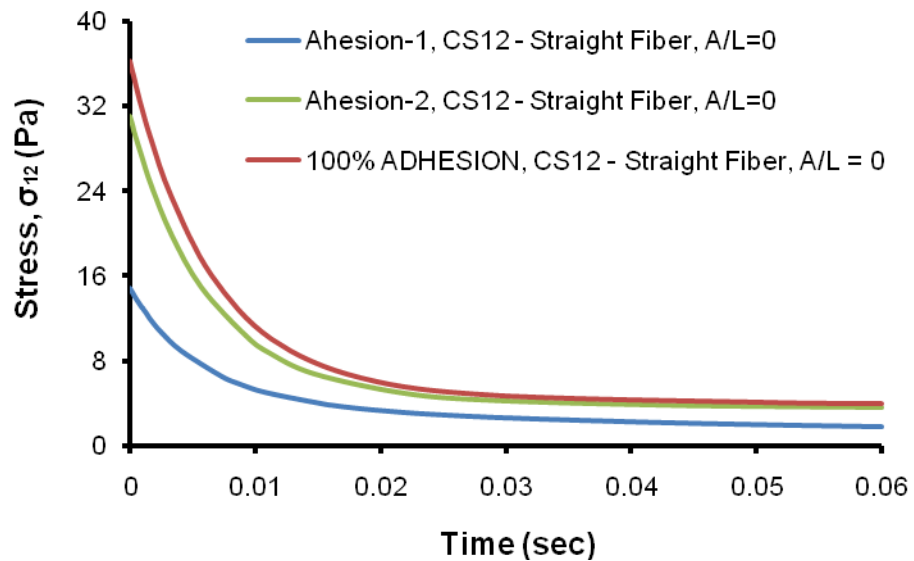


Figure 20. Variation of shear stress with respect to time due to the applied constant strain in direction 1-2 with three different adhesion properties in a unidirectional brain unit cell model of $V_F/V=0.53$.

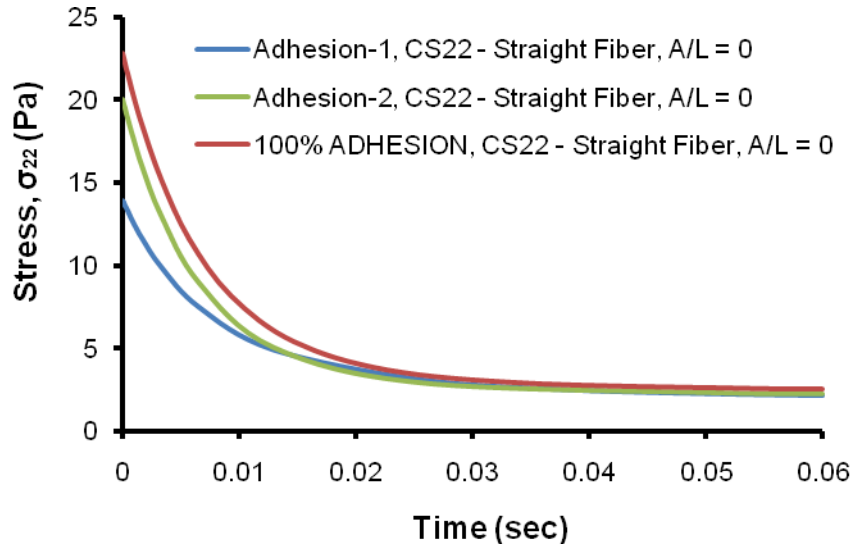


Figure 21. Variation of tensile stress with three different adhesion properties in axons, matrix, and brain composite tissue due to the applied constant strain in direction 2-2 in a unidirectional brain unit cell model of $V_F/V=0.53$.

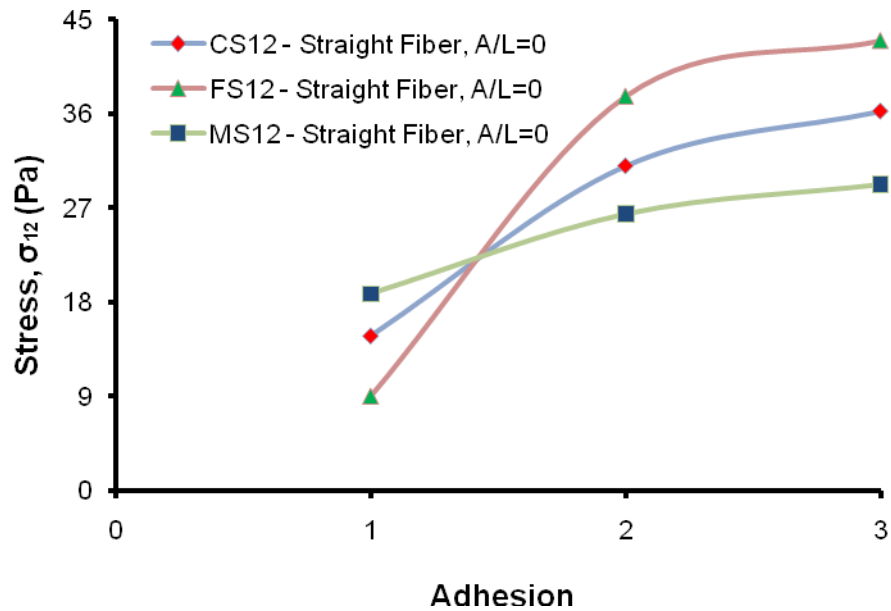


Figure 22. Variation of stiffness with three different adhesion properties in axons, matrix, and brain composite tissue due to the applied constant strain in direction 1-2 in a unidirectional brain unit cell model of $V_F/V=0.53$.

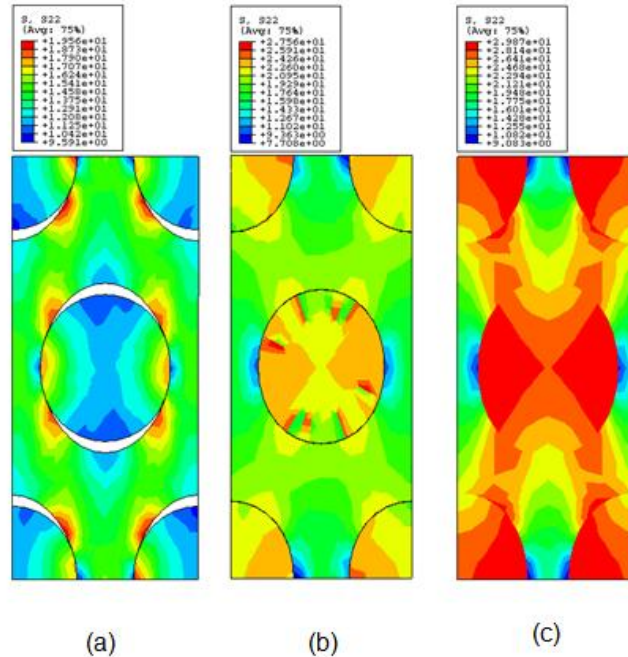


Figure 23. Illustration of the tensile stresses (S_{22}) developed in the (a) unidirectional tissue unit cell with A_1 (weak) adhesion; (b) unidirectional tissue unit cell with A_2 (strong) adhesion; and (c) unidirectional tissue unit cell with 100% bonding between axon and matrix when subjected to an average constant strain of 0.3% along 2-2 direction.

As the adhesion property changes from A_1 to A_3 , the axon material tends to be stiffer than the matrix and when the adhesion property changes from A_3 to A_1 , the matrix material tends to be stiffer than axons (Figure 20). Also for viscous behavior, similar trend is observed when the adhesion property changes from A_1 to A_3 with the axon material to be more viscous than the matrix and when the adhesion property changes from A_3 to A_1 , the matrix material tends to be more viscous than axons (Figure 20, 24). When observed with one fixed adhesion property, the stiffness and viscous behavior of brain tissue lies somewhere between axons and matrix (Figure 22). Similar impact has been observed for the overall brain composite tissue behavior. The stiffness and viscous behavior is high in the composite brain tissue with A_3 adhesion property and less with A_1 adhesion property (Figure 22). Similar trends for stiffness and viscous behavior are seen

for the transverse loading (Figure 21) and compressive loading (Figure 25) in direction 2-2. From Figure 23, for L-2 it can be inferred that there is an impact on the stiffness and viscous behavior on the brain tissue but the impact is not as significant as observed for L-4. From Figure 25, one interesting observation that can be found is that there is no much big impact of adhesion on the viscous behavior of brain unit cell model under compressive loading in 2-2 direction but there is an impact on the stiffness of the brain composite unit cell with the three different adhesion properties which is obvious as the adhesion strength changes. For all the load cases, the stiffness and viscous behavior of the brain composite unit cell follows the same trend for the three different adhesion properties and the stiffness and viscous behavior of the brain composite unit cell falls somewhere between the axon and matrix behavior based on the adhesion property.

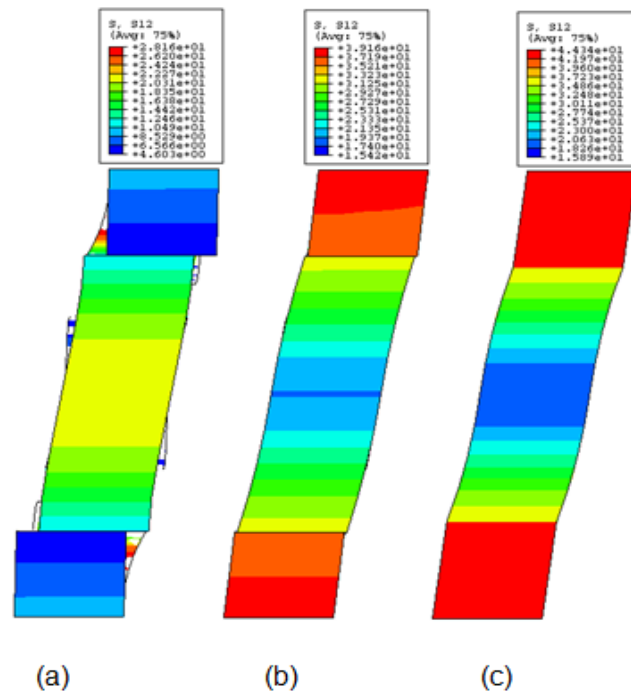


Figure 24. Illustration of the shear stresses (S_{12}) developed in the (a) unidirectional tissue unit cell with A_1 (weak) adhesion; (b) unidirectional tissue unit cell with A_2 (strong) adhesion; and (c) unidirectional tissue unit cell with 100% bonding between axon and matrix when subjected to an average constant strain of 0.3% along 1-2 direction.

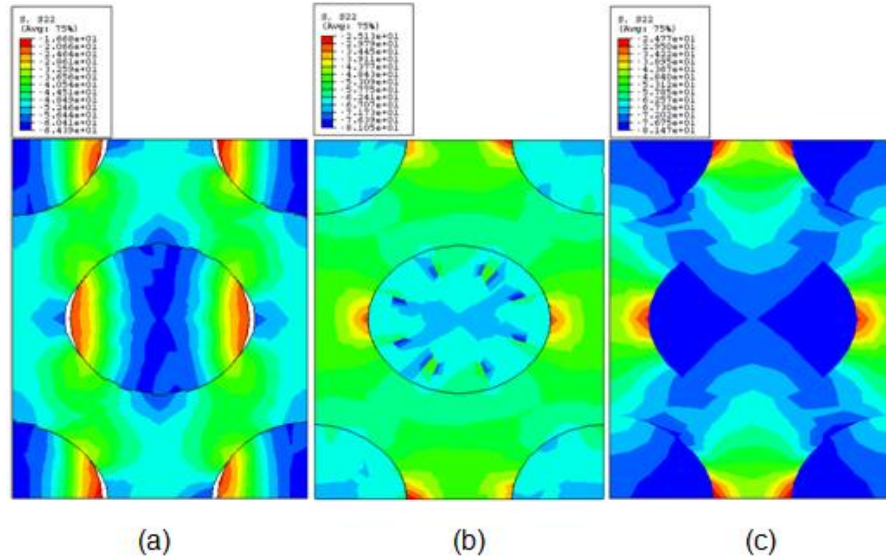


Figure 25. Illustration of the compressive stresses (S_{22}) developed in the (a) unidirectional tissue unit cell with A_1 (weak) adhesion; (b) unidirectional tissue unit cell with A_2 (strong) adhesion; and (c) unidirectional tissue unit cell with 100% bonding between axon and matrix when subjected to an average constant strain of 0.3% along 2-2 direction.

7.2 Impact of Adhesion on the Viscous Behavior of Axons and Matrix in a Brain

Composite Unit Cell with a Constant Waviness (A/L) of 1.0684 Using Bilinear Traction Separation Based Cohesive Zone

As discussed earlier, the adhesion strength is not the same in all the sections of the brain. In this section, the waviness is kept constant and the effect of different adhesion strengths on the stiffness and viscous behavior on the brain unit cell is studied using cohesive zone method for each load case. The wavy model implemented for this study is of amplitude/wavelength (A/L) of 1.0684. For the ease of calculations and faster convergence, we have implemented single mode bilinear cohesive zone behavior in this study [74]. The wavy brain composite unit cell with hexagonal packing is subjected to

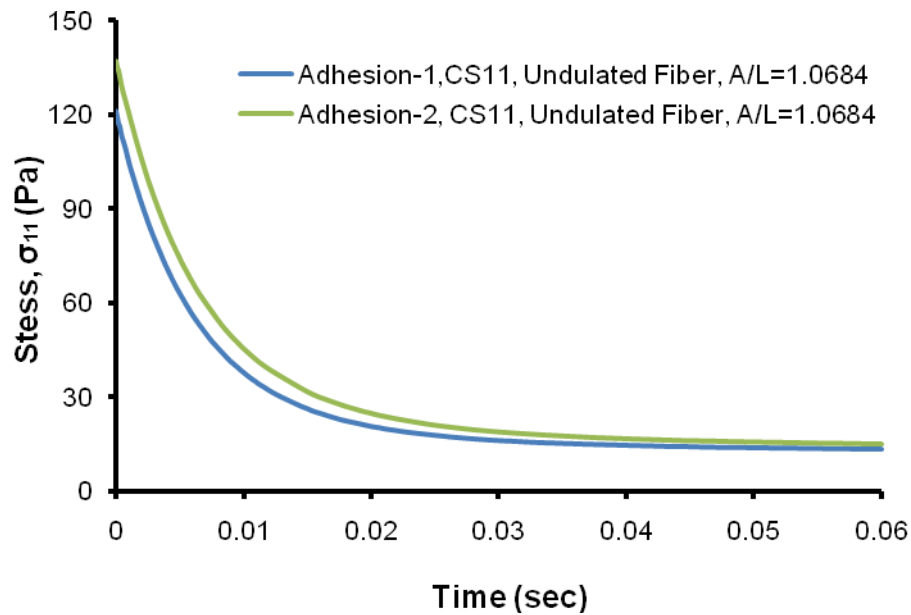


Figure 26. Variation of axial stress with respect to time due to the applied constant strain in direction 1-1 with two different adhesion properties in a brain unit cell model with waviness ($A/L=1.0684$) of $V_F/V=0.53$.

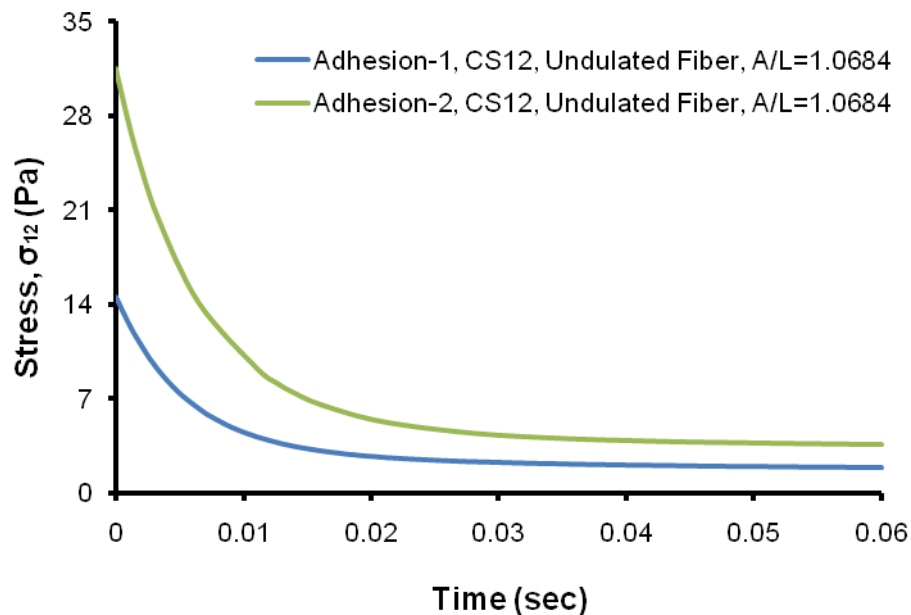


Figure 27. Variation of shear stress with respect to time due to the applied constant strain in direction 1-2 with two different adhesion properties in a brain unit cell model with waviness ($A/L=1.0684$) of $V_F/V=0.53$.

four different load cases which comprises of tensile loading in 1-1 direction (Load Case-1), compressive loading in 1-1 direction (Load Case-3), tensile loading in 2-2 direction (Load Case-2) and shear loading in 1-2 direction (Load Case-5).

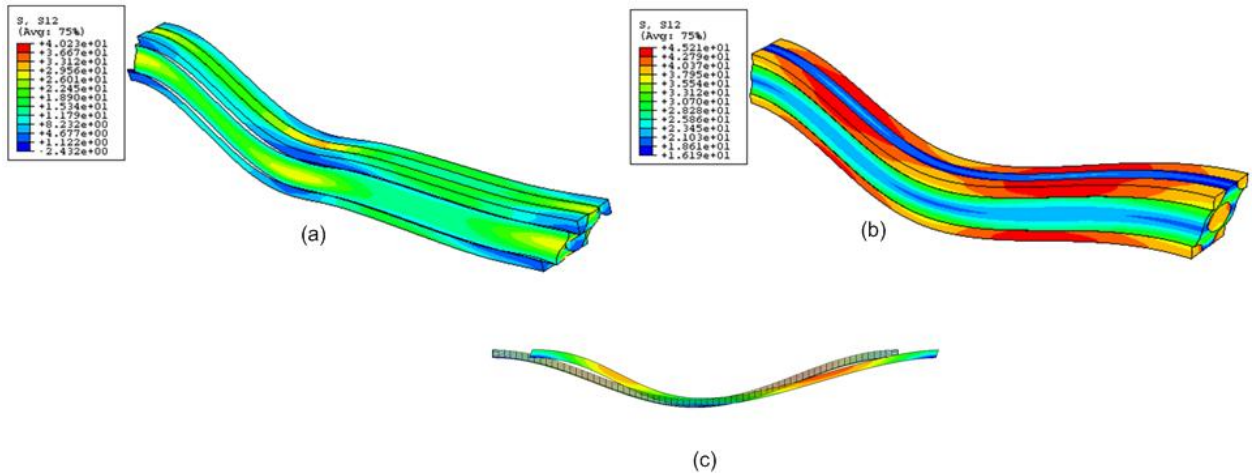


Figure 28. Illustration of the shear stresses (S_{12}) developed in the (a) tissue unit cell with undulation, $A/L=1.0684$ with A_1 (weak) adhesion; (b) tissue unit cell with undulation, $A/L=1.0684$ with A_2 (strong) adhesion when subjected to an average constant strain of 0.3% along 1-2 direction, which is perpendicular to the fiber direction (load case 5). The deformed shape of the axon with respect to its original shape is also shown in (c).

The above load cases represent almost all possible load scenarios during brain injury at microscopic level in which adhesion has a dominant role. In brain composite unit cell with unidirectional axon model, loading in longitudinal direction (Load case-1) did not have any significant impact on the overall stress distribution in axon or matrix. However, for wavy models both axon and matrix have an impact due to longitudinal loadings. Since in wavy models, axons are oriented over a curvature in a local direction, the global stresses should not remain constant. From the Fig. 26, the brain unit cell wavy models

with different adhesion when subjected to axial loading (L-1) in 1-1 direction had a significant impact on the stiffness and viscous behavior of the brain composite model. It can be observed that, with increase in adhesion strength, the stiffness and viscous behavior is high in the composite brain tissue with A_2 adhesion property and less with A_1 adhesion property (Figure 26). From the Fig. 29, a similar trend has been observed when the brain unit cell model has been subjected to compressive loading in 1-1 direction. One interesting thing is that the stiffness of the brain composite model for all the adhesion strengths in the compressive loading is high when compared to axial loading in the same direction under constant strain which implies that the tissue material is stiffer in compressive loading than axial loading. Another interesting observation is that the change in the stiffness and viscous behavior of the wavy unit cell is more significant with different adhesion strengths when compared to the axial loading in the same direction. From the Fig. 27, the wavy brain unit cell models with different adhesion when subjected to shear loading in 1-2 direction had a very high impact on the stiffness and viscous behavior of the brain composite model. It can be observed that, with increase in adhesion strength from A_1 to A_2 , the stiffness change is around 100% for a constant waviness (A/L) of 1.0684. A similar trend has been observed for the viscous behavior of the brain composite unit cell under shear loading in 1-2 direction and the change in viscous behavior is quite significant with increase in adhesion strength (Figure 28). For all the load cases subjected to wavy unit cell with different adhesion strengths, the stiffness and viscous behavior of the brain composite unit cell follows the same trend as explained above. The stiffness and viscous behavior of the brain composite wavy unit cell falls somewhere between the axon and matrix behavior depending upon the adhesion strength.

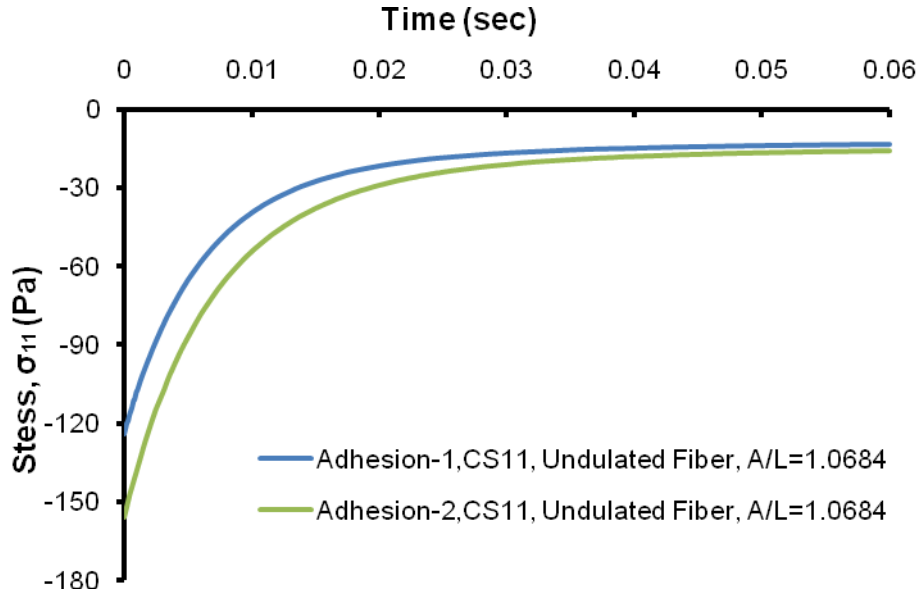


Figure 29. Variation of compressive stress with respect to time due to the applied constant strain in direction 1-1 with two different adhesion properties in a brain unit cell model with waviness ($A/L=1.0684$) of $V_F/V=0.53$.

7.3 Impact of Waviness on the Viscous Behavior of Axons and Matrix in a Brain

Composite Unit Cell with a Constant Adhesion Strength (A_1) Using Bilinear Traction Separation Based Cohesive Zone

The human brain consists of different sections like white matter, grey matter etc., and the waviness is not the same in all the sections of the brain. In this section, the adhesion strength is kept constant and the effect of different waviness on the stiffness and viscous behavior on the brain unit cell is studied using cohesive zone method for each load case. The results are quite different when compared to the results in section 7.2 as the constant parameter changes. The wavy models implemented for this study are of amplitude/wavelength (A/L) of 1.0684, 1.1310 and 1.1947. For the ease of calculations and faster convergence, we have implemented single mode bilinear cohesive zone

behavior in this study [74]. The wavy brain composite unit cell with hexagonal packing is subjected to the same load cases as mentioned in section 7.2. From the Fig. 30, the brain unit cell wavy models with different waviness when subjected to axial loading (L-1) in 1-1 direction had a significant impact on the stiffness and viscous behavior of the brain composite model under a constant adhesion strength. It can be observed that, with increase in waviness, the stiffness and viscous behavior is high in the composite brain tissue with high undulation and low in the composite brain tissue with least undulation under constant adhesion strength (Figure 31). It implies that regions in white matter such as brainstem in which axons are uniaxially oriented are weaker than regions of corona

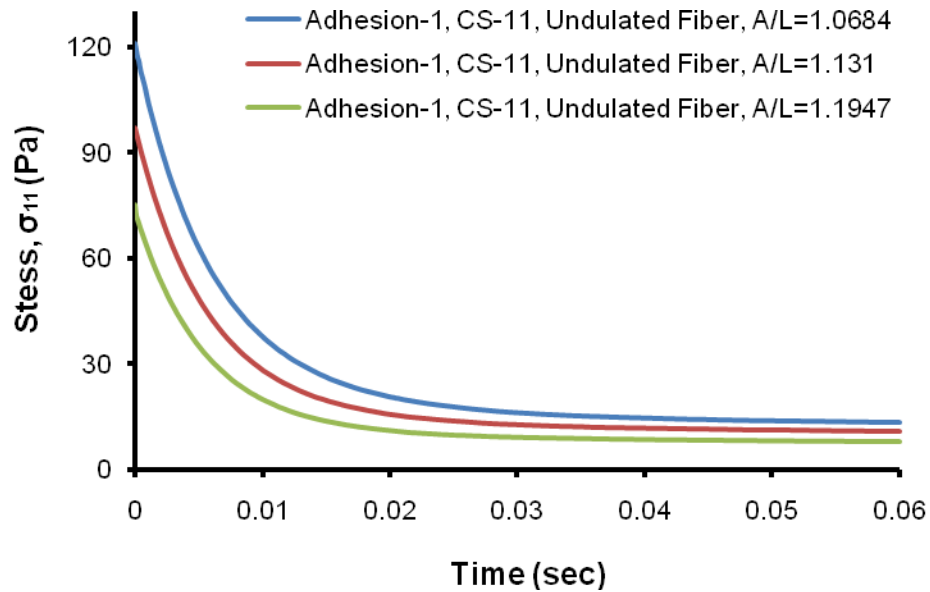


Figure 30. Variation of axial stress with respect to time due to the applied constant strain in direction 1-1 with three different waviness ($A/L=1.0684, 1.1310, 1.1947$) in a brain unit cell model with a weak adhesion property (A_1) of $V_F/V=0.53$.

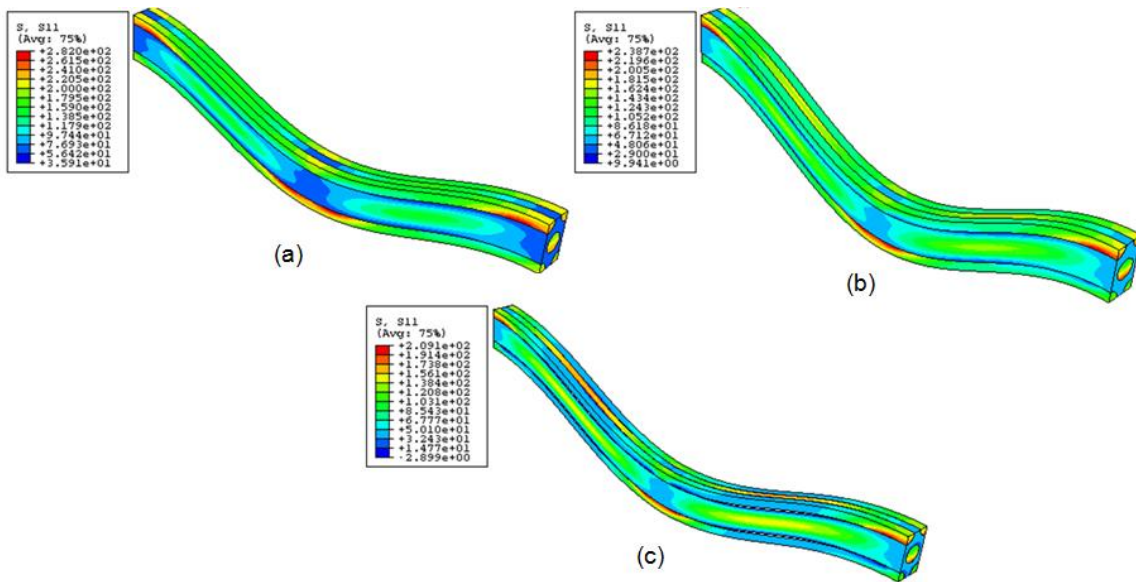


Figure 31. Illustration of the axial stresses (S_{11}) developed in the (a) tissue unit cell with undulation, $A/L=1.0684$ with A_1 (weak) adhesion; (b) tissue unit cell with undulation, $A/L=1.131$ with A_1 (weak) adhesion; and (c) tissue unit cell with undulation, $A/L=1.1947$ with A_1 (weak) adhesion when subjected to an average constant strain of 0.3% along longitudinal axon direction (load case 1).

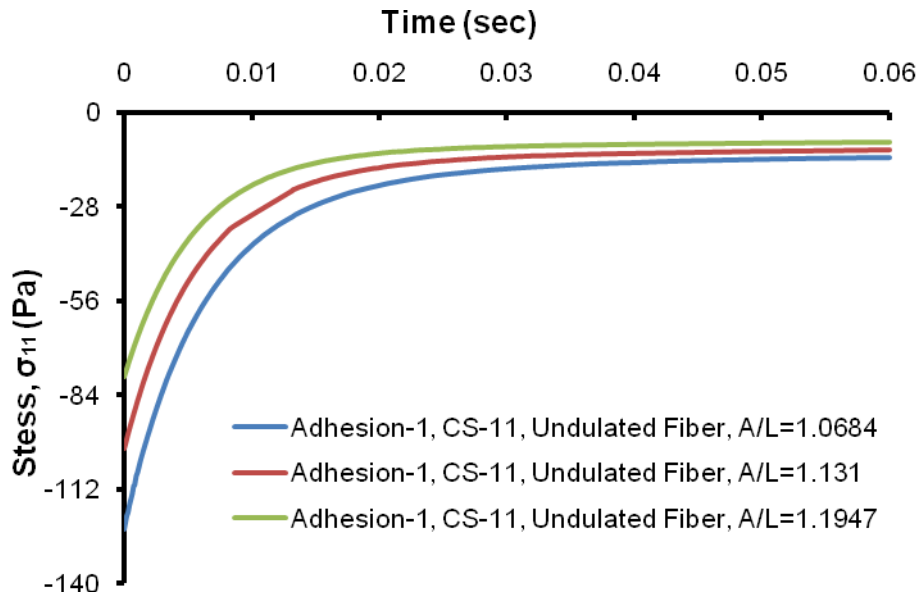


Figure 32. Variation of compressive stress with respect to time due to the applied constant strain in direction 1-1 with three different waviness ($A/L=1.0684$, 1.1310 , 1.1947) in a brain unit cell model with a weak adhesion property (A_1) of $V_F/V=0.53$.

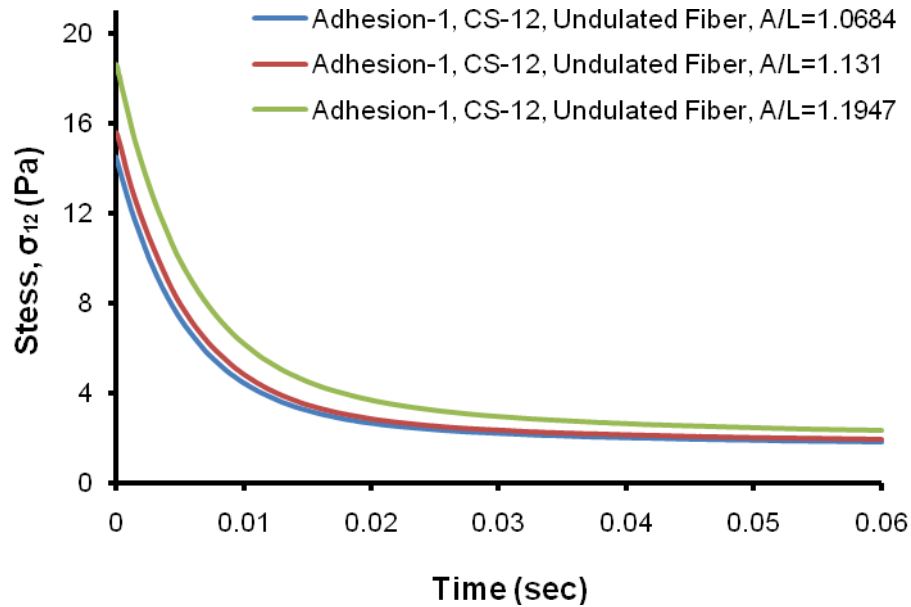


Figure 33. Variation of shear stress with respect to time due to the applied constant strain in direction 1-2 with three different waviness ($A/L=1.0684, 1.1310, 1.1947$) in a brain unit cell model with a weak adhesion property (A_1) of $V_F/V=0.53$.

radiata in which axons have high undulations. From Fig 26 & 30, one can infer by looking at the difference in percentage values of stiffness and viscous behavior that the effect of waviness under constant adhesion strength is much more significant when compared to the effect of adhesion under constant waviness for the respective load case (L-1). Similar trends have been observed in other load cases as well. From the Fig. 33, the brain unit cell model with different undulations when subjected to shear loading in 1-2 direction had an impact on the stiffness and viscous behavior of the brain composite model but impact of waviness is not as significant as we observed by the impact of adhesion strength in section 7.2. From Fig 27 & 33, one can infer by looking at the percentage difference in all the values of stiffness and viscous behavior that the effect of waviness under constant adhesion strength is less significant when compared to the effect

of adhesion under constant undulation for the respective load case. Similar trend has been observed for compressive loading (Figure 32). For all the load cases, looking at the variation in percentage values, it can be inferred that the waviness has a significant effect on the stiffness and viscous behavior of the brain tissue under specific adhesion strength.

CHAPTER 8. CONCLUSIONS AND SUGGESTIONS FOR FURTHER RESEARCH

8.1 *Conclusions*

To account for the impact of adhesion on the material behavior of composites and brain tissue a micromechanical computational model was introduced to simulate the composite fiber/matrix and Brain Axon/ECM structure by considering the cohesive zone between the composite constituents. In this study, we successfully incorporated the adhesion behavior inside the micromechanical model to determine the material response of the composite material and brain material for all possible loading scenarios.

For composites by implementing this micromechanical model it was observed that initial stiffness, strength and constant stiffness phase after failure of the cohesive zone can be characterized. Specific loading scenarios have been analyzed where adhesion has a major impact on the overall mechanical response of the composites. In this study for all the loading scenarios, we have observed that in all stress-strain plots there exists a point where all the three constituent's (fiber, matrix and composite) stresses are equal. This kind of composite behavior is also observed in Inglis et.al (2005). By this we can conclude that till this threshold point, fiber is the major load carrier and after that point stresses in fiber relax and matrix becomes the major load carrier. The tensile, compressive and shear strength evaluated by using this micromechanics tool are comparable with the published results. This micromechanical cohesive zone model has also been implemented to characterize the impact of wavy fibers on the overall composite response. For wavy composite models, we have studied that compressive strength is more

when compared longitudinal strength in same direction which means that the introduction of more wavy fibers will decrease the overall composite stiffness and strength in longitudinal compression and transverse directions. However it is observed composite materials with more wavy fiber distribution will result in a stronger material for shear. Also, it is studied that the wavy composite model has more tensile strength when compared to shear strength in same direction. The strength and initial stiffness of composite material for all the load cases evaluated using this micromechanics tool has been compared and all the values lie in the range of the available experimental material properties in the literature. A significant difference in the composite behavior has been observed when two different cohesive zone laws have been implemented which infers that shape of the softening zone is also an important factor in addition to initial stiffness and peak stress in cohesive zone law. The major difference observed while implementing the bi-linear and exponential traction-separation cohesive zone laws is that the peak stress attained by the composite has shifted more than twice in the case of exponential cohesive zone law. Based on the stress-strain plots of the composite from the experimental results, proper cohesive zone law can be determined.

In the case of brain material, by implementing this micromechanical model it was observed that stiffness and viscous behavior of the brain tissue can be implemented under different modes of injuries. A significant impact in the brain tissue due to adhesion strength has been observed under different loading scenarios. This micromechanical cohesive zone model has also been implemented to study the impact of wavy axons on the overall stiffness and viscous behavior of the brain tissue under three different adhesion strengths. With increase in adhesion, the axon material tends to be stiffer than

the matrix. Similar trend has been studied for viscous behavior of axons and matrix. When observed with one fixed adhesion property, the stiffness and viscous behavior of brain tissue lies somewhere between axons and matrix. With increase in adhesion property, the stiffness and viscous behavior of the overall composite brain tissue also increases. One interesting observation that can be found is that there is no much big impact of adhesion on the viscous behavior of brain unit cell model under compressive loading in transverse direction. The stiffness of the brain composite model for all the adhesion strengths in the compressive loading is high when compared to axial loading in the same direction under constant strain which implies that the tissue material is stiffer in compressive loading than axial loading. Another interesting observation is that the change in the stiffness and viscous behavior of the wavy unit cell is more significant with different adhesion strengths when compared to the axial loading in the same direction. The local stress and strain and distributions were also studied within a repeating unit cell. In this research analysis, we have also studied that the axons undulations also has a significant impact on the stiffness and viscous behavior in fiber direction under specific adhesion strength. It has been observed that with constant adhesion strength in longitudinal direction as waviness increases, the stiffness and viscous behavior also increases in the composite brain tissue. It implies that regions of white matter such as brainstem in which axons are uniaxially oriented are weaker in longitudinal direction when compared to regions of corona radiata in which axons have high undulations. It has been also been concluded that the effect of waviness under constant adhesion strength is less significant when compared to the effect of adhesion under constant undulation.

8.2 *Suggestions for Further Research*

The study of impact of adhesion in composites and brain tissue can be continued with this micromechanical approach by using different traction separation data. The traction separation data for composites can be determined with experimental pull out tests. In order to predict the precise effect of adhesion on different regions of brain tissue, accurate experimental traction separation model and data needs to be determined. With any available experimental traction separation data for brain tissue, we can study the actual mechanical behavior of different regions of brain tissues. We have studied this micromechanical model for composites and brain tissue by using elastic and viscoelastic materials for fiber and matrix. The research can be continued by studying the impact of adhesion using material properties like hyperelastic, hyperviscoelastic for fiber and matrix to evaluate the overall response of the composite and brain tissue.

REFERENCES

- [1] Brown HR. The adhesion between polymers. *Annual Review of Material Science* 1991;21:463-89.
- [2] Swaminathan S, Pagano NJ, Ghosh S. Analysis of Interfacial Debonding in three-dimensional Composite Microstructures. *J Engng Mater Tech* 2006;128:96-106.
- [3] Mat J. Pultruded Carbon Fiber/Vinyl Ester Composites Processed with Different Fiber Sizing Agents. Part I: Processing and Static Mechanical Performance. *Civ Engng* 2005;17(3):320-333.
- [4] Jayaraman K, Reifsnider KL and Swain RE. Elastic and thermal effects in the interphase: part II. Comments on modeling studies. *J of Composites Technology & Research* 1993;15(1):14-22.
- [5] Benveniste Y. On the Effect of Debonding on the Overall Behavior of Composite Materials *Mech Mater* 1985;3:349-358.
- [6] Hashin Z. Thermoelastic Properties of Fiber Composites with Imperfect Interface. *Mech Mater* 1990;8:333-348.
- [7] Needleman A. An Analysis of Decohesion Along an Imperfect Interface. *Int J Fract* 1990;42:21-40.
- [8] Needleman A. Micromechanical Modeling of Interfacial Decohesion. *Ultramicroscopy* 1992;40: 203-14.
- [9] Tvergaard V. Effect of Fiber Debonding in a Whisker-Reinforced Metal. *Mater Sci Eng, A* 1990;125: 203-213.
- [10] Ghosh S, Ling Y, Majumdar BS and Kim R. Interfacial Debonding in Multiple Fiber-Reinforced Composites. *Mech Mater* 2000;32:561-591.
- [11] Foulk JW, Allen DH and Helms KLE. Formulation of a Three-Dimensional Cohesive Zone Model for Application to a Finite Element Algorithm. *Comput Methods Appl Mech Eng* 2000;183:51-66.
- [12] Allen DH, Jones RH and Boyd JG. Micro-Mechanical Analysis of Continuous Fiber Metal Matrix Composite Including the Effects of Matrix Visco-Plasticity and Evolving Damage. *J Mech Phys Solids* 1994;42:502-529.
- [13] Lissenden CJ and Herakovich C T. Numerical Modeling of Damage Development and Viscoplasticity in Metal Matrix Composites. *Comput Methods Appl Mech Eng* 1995;125:289-303.
- [14] Geubelle PH. Finite Deformation Effects in Homogeneous and Interfacial Fracture. *Int J Solids Struct* 1995;32:1003-1016.
- [15] Camacho GT and Ortiz M. Computational Modeling of Impact Damage in Brittle Materials. *Int J Solids Struct* 1996;33:2899-2938.

- [16] Ortiz M and Pandolfi A. Finite-Deformation Irreversible Cohesive Element for Three-Dimensional Crack-Propagation Analysis. *Int J Numer Methods Eng* 1999;44:1267–1282.
- [17] Scheider Ingo. Cohesive Model for Crack Propagation Analyses of Structures with Elastic-Plastic Material Behavior: Foundations and Implementation. GKSS Research Center, Geesthacht 2001.
- [18] Segurado Javier and LLorca Javier. A New Three-Dimensional Interface Finite Element to Simulate Fracture in Composites. *Int J Solids Struct* 2004;41:2977–2993.
- [19] Ananth CR and Chandra N. Numerical modeling of fiber push-out test in metallic and intermetallic matrix composites–Mechanics of the failure processes. *J of Composite Materials* 1995a;29(11):1488–1514
- [20] Chandra N and Ananth CR. Analysis of interfacial behavior in MMCS and IMCS using thin-slice push-out tests. *Composite Science and Technology* 1995b;54(1):87–100.
- [21] Naik A, Abolfathi N, Karami G and Ziejewski M. Micromechanical Viscoelastic Characterization of Fibrous Composites. *J of Composite Materials* 2008;42(12): 1179-1204.
- [22] Sanes, J. R. and Yamagata, M. (1999). Formation of lamina-specific synaptic connections. *Curr. Opin. Neurobiol.* 9, 79-87.
- [23] Yamagata, M., Sanes, J. R. and Weiner, J. A.(2003). Synaptic adhesion molecules. *Curr. Opin. Cell Biol.* 5, 621-632.
- [24] Washbourne, P., Dityatev, A., Scheiffele, P., Biederer, T., Weiner, J. A., Christopherson, K. S. and El-Husseini, A. (2004). Cell adhesion molecules in synapse formation. *J. Neurosci.* 42, 9244-9249.
- [25] Brown, E.J., 1997. Adhesive interactions in the immune system. *Trends Cell Biol.* 7, 289–295. Benveniste Y. On the Effect of Debonding on the Overall Behavior of Composite Materials *Mech Mater* 1985;3:349–358.
- [26] Gimbrone, M.A., Nagel, T., Topper, J.N., 1997. Biomechanical activation: an emerging paradigm in endothelial adhesion biology. *J. Clin. Invest.* 99, 1809–1813.
- [27] Gumbiner, B.M., 1996. Cell adhesion: the molecular basis of tissue architecture and morphogenesis. *Cell* 84, 345–357.
- [28] Geiger, B., Bershadsky, A., 2001. Assembly and mechanosensory function of focal contacts. *Curr. Opin. Cell Biol.* 13, 584–592.
- [29] Wayner, E.A., Orlando, R.A., Cheresch, D.A., 1991. Integrins alpha v beta 3 and alpha v beta 5 contribute to cell attachment to vitronectin but differentially distribute on the cell surface. *J. Cell Biol.* 113, 919–929.

- [30] Tawil, N., Wilson, P., Carbonetto, S., 1993. Integrins in point contacts mediate cell spreading: factors that regulate integrins accumulation in point contacts vs. focal contacts. *J. Cell Biol.* 120, 261–271.
- [31] Wehrle-Haller, B., Imhof, B.A., 2002. The inner lives of focal adhesions. *Trends Cell Biol.* 12, 382–389.
- [32] Gracheva, M.E., Othmer, H.G., 2004. A continuum model of motility in ameboid cells. *Bull. Math. Biol.* 66, 167–193.
- [33] Sengers, B.G., Taylor, M., Please, C.P., Oreffo, R.O.C., 2007. Computational modelling of cell spreading and tissue regeneration in porous scaffolds. *Biomaterials* 28, 1926–1940.
- [34] Zhu, C., 2000. Kinetics and mechanics of cell adhesion. *J. Biomech.* 33, 23–33.
- [35] Zhu, C., Bao, G., Wang, N., 2000. Cell mechanics: mechanical response, cell adhesion, and molecular deformation. *Annu. Rev. Biomed. Eng.* 2, 189–226.
- [36] Evans, E.A., 1985a. Detailed mechanics of membrane-membrane adhesion and separation. I. Continuum of molecular cross-bridges. *Biophys. J.* 48, 175–183.
- [37] Evans, E.A., 1985b. Detailed mechanics of membrane-membrane adhesion and separation. II. Discrete kinetically trapped molecular crossbridges. *Biophys. J.* 48, 185–192.
- [38] Ward, M.D., Hammer, D.A., 1993. A theoretical analysis for the effect of focal contact formation on cell-substrate attachment strength. *Biophys. J.* 64, 936–959.
- [39] Dembo, M., Torney, D.C., Saxman, K., Hammer, D., 1988. The reactionlimited kinetics of membrane-to-surface adhesion and detachment. *Proc. R. Soc. Lond. Ser. B* 234, 55–83.
- [40] Ward, M.D., Dembo, M., Hammer, D.A., 1994. Kinetics of cell detachment: peeling of discrete receptor clusters. *Biophys. J.* 67, 2522–2534.
- [41] Evans, E., Ritchie, K., 1997. Dynamic strength of molecular adhesion bonds. *Biophys. J.* 72, 1541–1555.
- [42] Marshall, B.T., Long, M., Piper, J.W., Yago, T., McEver, R.P., Zhu, C., 2003. Direct observation of catch bonds involving cell-adhesion molecules. *Nature* 423, 190–193.
- [43] Marshall, B.T., Sarangapani, K.K., Lou, J.H., McEver, R.P., Zhu, C., 2005. Force history dependence of receptor–ligand dissociation. *Biophys. J.* 88, 1458–1466.

- [44] Hanley, W., McCarty, O., Jadhav, S., Tseng, Y., Wirtz, D., Konstantopoulos, K., 2003. Single molecule characterization of P-selectin/ligand binding. *J. Biol. Chem.* 278, 10556–10561.
- [45] Bayas, M.V., Schulten, K., Leckband, D., 2003. Forced detachment of the CD2-CD58 complex. *Biophys. J.* 84, 2223–2233.
- [46] Buehler, M.J., Yao, H., Gao, H., Ji, B., 2006. Cracking and adhesion at small scales: atomistic and continuum studies of flaw tolerant nanostructures. *Modell. Simul. Mater. Sci. Eng.* 14, 799–816.
- [47] Gao, H., Ji, B., 2003. Modeling fracture in nanomaterials via a virtual internal bond method. *Eng. Fract. Mech.* 70, 1777–1791.
- [48] Gao, H., Yao, H., 2004. Shape insensitive optimal adhesion of nanoscale fibrillar structures. *Proc. Natl. Acad. Sci. USA* 101, 7851–7856.
- [49] Gao, H., Ji, B., Jager, I.L., Arzt, E., Fratzl, P., 2003. From the cover: materials become insensitive to flaws at nanoscale: lessons from nature. *Proc. Natl. Acad. Sci. USA* 100, 5597–5600.
- [50] Ji, B., Gao, H., 2004a. Mechanical properties of nanostructure of biological materials. *J. Mech. Phys. Solids* 52, 1963–1990.
- [51] Yao, H., Gao, H., 2006. Mechanics of robust and releasable adhesion in biology: bottom-up designed hierarchical structures of gecko. *J. Mech. Phys. Solids* 54, 1120–1146.
- [52] Dong Kong., Baohua Ji., Lanhong Dai., 2007. Nonlinear Mechanical Modeling of cell adhesion. *J. Theoretical Biology.* 250, 75–84.
- [53] Martinez, E.J.P., Lanir, Y., Einav, S., 2004. Effects of contact-induced membrane stiffening on platelet adhesion. *Biomech. Model. Mechanobiol.* 2, 157–167.
- [54] Lotz, M. M., C. A. Burdsal, H. P. Erickson, and D. R. McClay. 1989. Cell adhesion to fibronectin and tenascin: quantitative measurements of initial binding and subsequent strengthening response. *J. Cell Biol.* 109: 1795-1805.
- [55] Toshiaki Sakisaka and Yoshimi Takai. 2005. Cell adhesion molecules in the CNS. *J. Cell Science.* 118, 5407-5410.
- [56] Hashin Z, Rosen BW. The elastic moduli of fiber-reinforced materials. *ASME Journal of Applied Mechanics* 1964;31:223–232.
- [57] Aboudi J. *Mechanics of Composite Materials, a Unified Micromechanical Approach.* Elsevier Science Publishers, Amsterdam, 1991.

- [58] Needleman A, Tvergaard V. Comparison of crystal plasticity and isotropic hardening predictions for metal-matrix composites. *ASME Journal of Applied Mechanics*, 1993;60:70–76.
- [59] Karami G and Garnich M. Effective Moduli and Failure Considerations for Composite with Periodic Fiber Waviness. *J of Composite Structures* 2005;67(4):461-475.
- [60] Adams DF and Crane DA. Finite element micromechanical analysis of a unidirectional composite including longitudinal shear loading. *Computer and Structures*, 1984;18:1163–1165.
- [61] Brinson LC and Lin WS. Comparison of micromechanics methods for effective properties of multiphase viscoelastic composites. *Composite Structures* 2003;41:353-367.
- [62] Fisher FT and Brinson LC. Viscoelastic interphase in polymer-matrix composites: theoretical models and finite element analysis. *Composite Science and Technology* 2003;61:731-748.
- [63] Arbogast, K. B. and Margulies, S. S. (1999). A fiber-reinforced composite model of the viscoelastic behavior of the brainstem in shear, *J of Biomechanics*, 32, 865–870.
- [64] Stecenko T and Piggott MR. Fiber Waviness and Other Mesostructures in Filament Wound Materials. *J of Reinforced Plastics and Composites* 1997;16:1659–1674.
- [65] Hsiao HM and Daniel IM. Nonlinear Elastic Behavior of Unidirectional Composites with Fiber Waviness under Compressive Loading. *ASME Journal of Engineering Materials and Technology* 1996;118:561–570.
- [66] Gardner SD, Pittman CU Jr. and Hackett RM. Residual thermal stresses in filamentary polymer–matrix composites containing an elastomeric interphase. *Journal of Composite Materials* 1993;27(8):830–860.
- [67] Termonia Y. Fiber coating as a means to compensate for poor adhesion in fiber-reinforced materials. *Journal of Materials Science* 1990;25:103–106.
- [68] Munz M, Sturm H, Schulz E and Hinrichsen G. The scanning force microscope as a tool for the detection of local mechanical properties within the interphase of fiber reinforced polymers. *Composites Part A* 1998;29A:1251–1259.
- [69] Thomason L. The interface region in glass fiber-reinforced epoxy resin. *Composites: 3. Characterization of fiber surface coatings and the interphase. Composites* 1995;26 :487–498.
- [70] Mai K, Mader E and Muhle M. Interphase characterization in composites with new non-destructive methods. *Composites Part A* 1998;29A:1111–1119
- [71] Bell, G.I., Dembo, M., Bongrand, P., 1984. Cell adhesion. Competition between nonspecific repulsion and specific bonding. *Biophys. J.* 45, 1051–1064.
- [72] Clarence E. Chan and David J. 2008. Odde Traction Dynamics of Filopodia on Compliant Substrates. *Science* Vol. 322. no. 5908, pp. 1687 – 1691.

- [73] Dikla Raz–Ben Aroush., Hanoch Daniel Wagner. 2006. Shear-Stress Profile along a Cell Focal Adhesion. *J. Adv. Mater.* 2006, 18, 1537–1540.
- [74] ABAQUS. Manual, Version 5.8, Habbit, Karlsson & Sorensen, Inc., USA, 2006.
- [75] Swaminathan S, Pagano NJ and Ghosh S. Analysis of Interfacial Debonding in Three-dimensional Composite Microstructures, *J. Engng. Mater. Tech* 2006b;128: 96–106.
- [76] Chandra N, Li H, Shet C and Ghonem H. Some Issues in the Application of Cohesive Zone Models for Metal-ceramic Interface. *Int. J. Solids Struct* 2002;39:2827–2855.
- [77] Li S and Ghosh S. Debonding in Composite Microstructures with Morphologic Variations. *International Journal of Computational Methods* 2004;1(1):21–149.
- [78] Kim S-H and Kim C-G. Optimal Design of Composite Stiffened Panel with Cohesive Elements using Micro-Genetic Algorithm. *Journal of Composite Materials* 2008;42(21):2259-2273.
- [79] Inglis HM, Geubelle PH, Matous K, Tan H and Huang Y. Cohesive Modeling of dewetting in particulate composites: micromechanics vs. multiscale finite element analysis. *J of Mechanics of Materials* 2007;39:580-595.
- [80] Kreculji DD, Stress Analysis in a Unidirectional Carbon/Epoxy Composite Material. *J of FME Transactions* 2008;36:127-132.
- [81] Kim BC and Lee DG. Development of spherical bearing with uni-directional carbon/epoxy composite. *J of composite Structures* 2008.
- [82] De Moura MFSF, Gonclaves JPM, Marques AT and De Castro PMST. Prediction of compressive strength of carbon-epoxy laminates containing delamination by using a mixed-mode damage model. *J of Composite Structures* 2000;50:151-157.
- [83] Robinson P, Galvanetto U, Tumino D, Belluci G and Violeau D. Numerical simulation of fatigue driven delamination using interface elements. *Int J for Numerical Methods in Engg* 2005;63:1824–1848.
- [84] Takashi I, Kazuo K and Shigeo K. Elastic Moduli of Carbon/Epoxy Composites and Carbon Fibers. *J of Composite Materials* 1977;11: 332-344.
- [85] Li S and Ghosh S. Debonding in Composite Microstructures with Morphologic Variations. *Int. J of Computational Methods* 2004;1(1):21–149.
- [86] Kim S-H and Kim C-G. Optimal Design of Composite Stiffened Panel with Cohesive Elements using Micro-Genetic Algorithm. *J of Composite Material* 2008;42(21):2259-2273.
- [87] Ferrant, M., Warfield, S., Nabavi, A., Jolesz, K. and Kikinis, F. (2000). Registration of 3D intraoperative MR images of the brain using a finite element biomechanical model, *MICCAI 2000 Proceedings, Pittsburg*, 19–28.

- [88] Skrinjar, O. M., Studholme, C., Nabavi, A. and Duncan, J. S. (2001). Steps toward a stereo-camera-guided biomechanical model for brain shift compensation, *Lect Notes in Comp Sci: IPMI 2001*, 183–189.
- [89] Meaney, D. F. (2003). Relationship between structural modeling and hyperelastic material behavior: application to CNS white matter, *Biomech Model Mechanobiol*, 1, 279–293.
- [90] Mendis, K. K., Stalnaker, R. and Advani, S. H. (1995). A constitutive relationship for large-deformation finite-element modeling of brain-tissue, *ASME J of Biomech Eng Trans*, 117, 279–285.
- [91] Wang, H.C. and Wineman, A.S. (1972). A mathematical model for the determination of viscoelastic behavior of brain in vivo oscillatory response, *J of Biomechanics*, 5, 431–46.
- [92] Karami G and Garnich M. Effective Moduli and Failure Considerations for Composite with Periodic Fiber Waviness. *J of Composite Structures* 2005;67(4):461-475.
- [93] Naik, A., Abolfathi, N., Karami, G. and Ziejewski, M. (2008). Micromechanical Viscoelastic Characterization of Fibrous Composites, *J of Composite Materials*, 42, 1179-1204.
- [94] Abolfathi, N., Naik, A., Sotudeh, M., Karami, G. and Ziejewski, M. (2009). A micromechanical procedure for characterization of the mechanical properties of brain white matter, *Computer Methods in Biomechanics and Biomedical Engineering*, 12(3), 249–262.
- [95] Sorensen BF and Jacobsen TK. Characterizing delamination of fiber composites by mixed mode cohesive laws. *J of Composites Science and technology*, 2008.